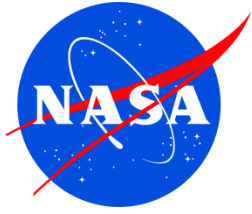


NASA/TM-2010-216132



C-9 and Other Microgravity Simulations Summary Report

*Report prepared by
Space Life Sciences Directorate
Human Adaptation and Countermeasures Division
NASA Johnson Space Center, Houston*

National Aeronautics and
Space Administration

Johnson Space Center
Houston, TX 77058

September 2010

THE NASA STI PROGRAM OFFICE . . . IN PROFILE

Since its founding, NASA has been dedicated to the advancement of aeronautics and space science. The NASA Scientific and Technical Information (STI) Program Office plays a key part in helping NASA maintain this important role.

The NASA STI Program Office is operated by Langley Research Center, the lead center for NASA's scientific and technical information. The NASA STI Program Office provides access to the NASA STI Database, the largest collection of aeronautical and space science STI in the world. The Program Office is also NASA's institutional mechanism for disseminating the results of its research and development activities. These results are published by NASA in the NASA STI Report Series, which includes the following report types:

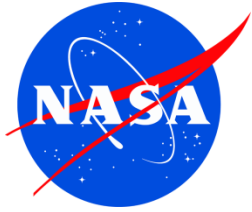
- **TECHNICAL PUBLICATION.** Reports of completed research or a major significant phase of research that present the results of NASA programs and include extensive data or theoretical analysis. Includes compilations of significant scientific and technical data and information deemed to be of continuing reference value. NASA's counterpart of peer-reviewed formal professional papers but has less stringent limitations on manuscript length and extent of graphic presentations.
- **TECHNICAL MEMORANDUM.** Scientific and technical findings that are preliminary or of specialized interest, eg, quick release reports, working papers, and bibliographies that contain minimal annotation. Does not contain extensive analysis.
- **CONTRACTOR REPORT.** Scientific and technical findings by NASA-sponsored contractors and grantees.
- **CONFERENCE PUBLICATION.** Collected papers from scientific and technical conferences, symposia, seminars, or other meetings sponsored or cosponsored by NASA.
- **SPECIAL PUBLICATION.** Scientific, technical, or historical information from NASA programs, projects, and mission, often concerned with subjects having substantial public interest.
- **TECHNICAL TRANSLATION.** English-language translations of foreign scientific and technical material pertinent to NASA's mission.

Specialized services that complement the STI Program Office's diverse offerings include creating custom thesauri, building customized databases, organizing and publishing research results . . . even providing videos.

For more information about the NASA STI Program Office, see the following:

- Access the NASA STI Program Home Page at <http://www.sti.nasa.gov>
- E-mail your question via the Internet to help@sti.nasa.gov
- Fax your question to the NASA Access Help Desk at (301) 621-0134
- Telephone the NASA Access Help Desk at (301) 621-0390
- Write to:
NASA Access Help Desk
NASA Center for AeroSpace Information
7115 Standard
Hanover, MD 21076-1320

NASA/TM-2010-216132



C-9 and Other Microgravity Simulations Summary Report

*Report prepared by
Space Life Sciences Directorate
Human Adaptation and Countermeasures Division
NASA Johnson Space Center, Houston*

National Aeronautics and
Space Administration

Johnson Space Center
Houston, TX 77058

September 2010

PREFACE

This document represents a summary of medical and scientific evaluations conducted aboard the C-9 and other NASA-contracted aircraft from June 2009 to June 2010. Included is a general overview of investigations manifested and coordinated by the Human Adaptation and Countermeasures Division. A collection of brief reports that describes tests conducted aboard NASA-sponsored aircraft follows the overview. Principal investigators and test engineers contributed significantly to the content of the report, describing their particular experiment or hardware evaluation. Although this document follows general guidelines, each report format may vary to accommodate differences in experiment design and procedures. This document concludes with an appendix that provides background information concerning the NASA Reduced Gravity Program.



Acknowledgments

The Space Life Sciences Directorate gratefully acknowledges the work of Sharon Hecht, Jacqueline M. Reeves, and Elisabeth Spector for their outstanding editing support and contributions to the overall quality of this annual summary report.

Available from:

NASA Center for AeroSpace Information
7115 Standard Drive
Hanover, MD 21076-1320
Phone: 301-621-0390 or
Fax: 301-621-0134

National Technical Information Service
5285 Port Royal Road
Springfield, VA 22161
703-605-6000

This report is also available in electronic form at <http://ston.jsc.nasa.gov/collections/TRS/>

**C-9 and Other Microgravity Simulations
Summary Report – September 30, 2010**

National Aeronautics and Space Administration
Lyndon B. Johnson Space Center

Prepared by: Wanda L. Thompson 8/31/10
Wanda L. Thompson, RN, BC, NMCC
Coordinator
JES Tech, LLC
Date

Noel C. Skinner 8/31/10
Noel C. Skinner, MS
Alternate Coordinator
Wyle Integrated Science and Engineering Group
Date

Approved by: Jeanie L. Nillen 8/31/10
Jeanie L. Nillen, MT(ASCP)
Manager
Human Adaptation and Countermeasures Group
Wyle Integrated Science and Engineering Group
Date

Approved by: Todd T. Schlegel 8/31/10
Todd T. Schlegel, MD
Technical Monitor
Human Adaptation and Countermeasures Division
Reduced Gravity Program
NASA Johnson Space Center
Date

Contents

	Page
Overview of Reduced Gravity Flight Activities Sponsored by the Human Adaptation and Countermeasures Division.....	1
Medical and Scientific Evaluations during Parabolic Flights.....	2
Education Outreach Program – Effects of Altered Gravity on Cellular Function.....	3
High-Accuracy Eye-movement Monitor	12
FASTRACK Program – Antimicrobial Polymers Project.....	16
Education Outreach Program – Space Motion Sickness and the Semicircular Canals of the Inner Ear	33
Appendix.....	A-1
Background Information about the C-9 and NASA Reduced Gravity Program	A-2

Acronyms

ACS	American Chemical Society
AFRL	Air Force Research Laboratory
Ag	silver
AgF	silver fluoride
AMME-TEDP	Antimicrobial Materials for Microgravity Environments Test Equipment Data Package
AMPP	Advanced Materials Processing Program
AO	acridine orange
AODC	acridine orange direct count
ASTM	American Society for Testing and Materials
ATP	adenosine triphosphate
AWRSDF	Advanced Water Recovery System Development Facility
BRIC	Biological Research in a Canister
BRIC-LED	Biological Research in a Canister-Light-emitting Diode
BSC	biological safety cabinet
CDC	change data capture
CO ₂	carbon dioxide
CPHS	Committee for the Protection of Human Subjects
Cr	chromium
DNA	deoxyribonucleic acid
ECLS	environmental control and life support
ERI	engineered roughness index
ESEM	environmental scanning electron microscopy
EtO	ethylene oxide
FAST	Facilitated Access to Space Environment for Technology Development and Training
fPOSS	fluorodecyl polyhedral oligomeric silsesquioxanes
HPC	heterotrophic plate count
ICP-AES	inductively coupled plasma atomic emission spectroscopy
IPP	integrated phase planning
IRB	Institutional Review Board
ISK	inverse Sharklet™
ISS	International Space Station
JSC	Johnson Space Center
KSC	Kennedy Space Center
L/D	live/dead
LSSC	launch services support contract
MESA	mathematics, engineering, science, and achievement
MPDFU	modified Petri dish fixation unit
Na ₂ CrO ₄	sodium chromate
NSTA	National Science Teachers Association
P	pilin peptide
PBS	phosphate buffered saline
PC	polycarbonate

PDFU	Petri dish fixation unit
PDMS	polydimethylsiloxane
PE	polyethylene
PET	polyethylene terephthalate
POSS	polyhedral oligomeric silsesquioxanes
ppb	parts per billion
QGA [™]	Quench-Gone Aqueous
RGO	Reduced Gravity Office
SAS	space adaptation syndrome
SEM	scanning electron microscopy
SM	smooth
SMS	space motion sickness
SPDFU	standard Petri dish fixation unit
SS	stainless steel
Ti	titanium
TSB	Trypticase [™] Soy Broth
USM	University of Southern Maine
UV	ultraviolet
WAD	work authorization document

Overview of Reduced Gravity Flight Activities
Sponsored by the Human Adaptation and Countermeasures Division

As a summary for the year, 4 weeks were specifically reserved for flights sponsored from June 2009 to June 2010. Seven flights with approximately 32 parabolas per flight were completed and the average duration of each flight was 2.1 hours. The Reduced Gravity Program coordinator assisted principal investigators and test engineers of 7 different experiments and hardware evaluations in meeting the necessary requirements for flying aboard the C-9 or another NASA-contracted aircraft and in obtaining the required seating and floor space. Support was provided to the Education Outreach Program during weeks in June and August 2009 and in April 2010. A large ground crew from the respective academic institutions supported the in-flight experiments. The number of seats supported and number of different tests flown by flight week are provided below:

Flight Week	Seats	No. Tests Flown	Sponsor
2009			
June 11–12	6	1	Education Outreach Program
August 11–14	35	4	FASTRACK
2010			
April 29–30	10	2	Education Outreach Program

Further flights will be added throughout the remainder of calendar year 2010 to accommodate customers as needs arise.

Medical and Scientific Evaluations during Parabolic Flights

TITLE

Education Outreach Program –
Effects of Altered Gravity on Cellular Function

FLIGHT DATES

June 11–12, 2009

PRINCIPAL INVESTIGATOR

John Pierce Wise, Sr., PhD, University of Southern Maine (USM), Portland, ME

COINVESTIGATORS

John P Wise, USM
Michael Browne, USM
Jane McKay, USM
Jennifer Brown, USM
Matthew Braun, USM
James Wise, USM
Catherine Wise, USM
Ryan Duffy, USM
Eben Estell, USM
Sandra Wise, USM
Kellie Joyce, USM
Michael Mason, PhD, USM



GOAL

To determine the effects of altered gravity on cellular function.

OBJECTIVES

To determine how altered gravity affects cellular function, we looked at three specific objectives:

1. Determine whether human genotoxic agents cause more damage to cells and deoxy-ribonucleic acid (DNA) in altered gravity than in normal gravity. The effects of altered gravity on the potency of human genotoxicants are not well understood. Last year we found that altered gravity increases damage induced by genotoxic chromate. Thus, this specific objective is to confirm the effects of altered gravity on DNA damage in comparison to normal gravity using an assay for chromosome damage.
2. Determine whether the change in the amount of chromosome damage is due to an increase in cellular uptake of chemicals by facilitated diffusion and phagocytosis in altered gravity: The ability of cells to take up chemicals in altered gravity is not well understood. This objective is to determine the effects of altered gravity on facilitated diffusion and phagocytosis using assays for ion uptake and particle internalization.
3. Determine whether the change in the amount of chromosome damage is due to inhibition of DNA repair mechanisms by altered gravity. The effects of altered gravity on DNA repair mechanisms are not well understood. This objective is to determine the effects of altered gravity on DNA repair relative to normal gravity, using an assay for DNA double-strand breaks.

METHODS AND MATERIALS

Overview

This hypothesis was tested by measuring the effects of known genotoxic chemicals in altered gravity (flight), and comparing the results to identical tests conducted in normal gravity (ground). To keep the cells alive, we took a mini-oven (kept at human body temperature 37°C [98°F]) on board the plane with us. The mini-oven was secured to the floor of the plane using a structure designed by SpaceWorks, Inc. (Grand Junction, CO). A cooler was attached on top of this structure to stop a few experiments at the end of flight. We used this cooler on our first flight but decided it was not important for this year's experiment. Our task on board the plane was to monitor the temperature and power. Collectively, the cooler-oven system (figure 1) worked very well for our experiments.

Figure 1. The "rig" used to maintain the cells in flight.



Cells and Cell Culture

The human lung cells were developed in the Wise Laboratory (Blankenship et al., 1997). These cells are fibroblasts immortalized with telomerase. The telomerase serves to extend the fibroblasts' life spans, but the cells otherwise function normally

and maintain normal responses to metals (Blankenship et al., 1997). The cells, which were maintained as adherent subconfluent monolayers (figure 2), were seeded 48 h before treatment to allow them to settle and resume normal growth. For our experiments the cells were grown in T-25 flasks (figure 3A) and on sealed slide chambers (figure 3B). All experiments were conducted on logarithmically growing cells. There is little concern for the lack of carbon dioxide (CO₂) gas exchange (an essential compound for cell growth) during the flight because the length of time without CO₂ exchange is insignificant.

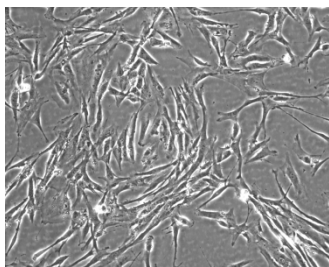
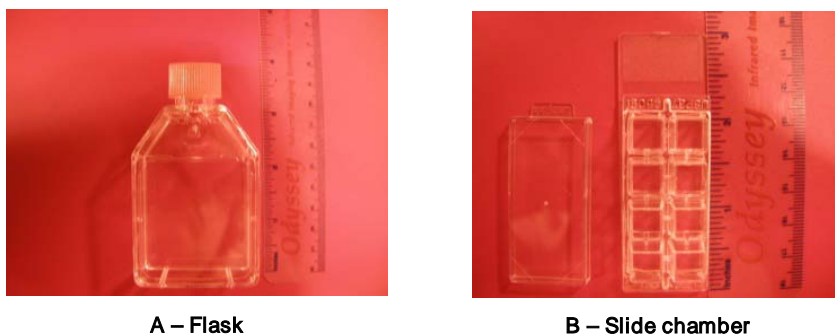


Figure 2. Human lung fibroblast cells under microscope.



A – Flask

B – Slide chamber

Figure 3. Pictures of cell culture tools.

Treatments

Sodium chromate (Na₂CrO₄) (CAS #7775-11-3, American Chemical Society (ACS) reagent minimum 98% purity) was used as a soluble hexavalent chromium salt, Cr(VI). Solutions of Na₂CrO₄ were prepared by: (1) measuring the desired amount of Na₂CrO₄; (2) dissolving the Na₂CrO₄ in double distilled water; and (3) filtering the solution through a 0.2-μm filter to sterilize the solution. We used 5 to 20-μM concentrations of Na₂CrO₄ as our laboratory has employed these methods with success (Xie et al., 2004).

We treated cells for varying times, as indicated under each specific objective. All treatments were done at the Bioscience Core Laboratory at the NASA Johnson Space Center before flight. Our experiments focused on using vitamin C and cold temperature to stop the treatments. For repair experiments, we used vitamin C to stop the Na₂CrO₄ treatment, allowing the cells' repair mechanisms to begin, because Na₂CrO₄ is a form of Cr(VI). Cr(VI) ions can enter the cell with the help of a protein in the plasma membrane (Wise et al., 2004). By contrast, trivalent chromium Cr(III) ions cannot enter the cell (Wise et al., 2004). By adding vitamin C, the Cr(VI) ions are reduced to Cr(III) ions outside the cell, thus preventing further chromium (Cr) uptake. Therefore, vitamin C prevents Cr ions from getting into the cell and causing more DNA damage (Xie et al., 2005; Crawford-Young, 2006; Tischler and Morey-Holton, 1993). Not only does this approach prevent uptake, but our laboratory has shown that this approach also prevents chromosome damage after Na₂CrO₄ exposure (Crawford-Young, 2006; Tischler and Morey-Holton, 1993). Vitamin C was dissolved in double distilled water before it was sterilized by filtering through a 0.2-μm filter. We used a 2-μM vitamin C co-treatment as our laboratory found that this concentration maximizes the amount of chromate reduction without inducing cytotoxicity (Crawford-Young, 2006).

The results of these experiments have implications for protecting the health of astronauts going on extended missions to the International Space Station (ISS), the Moon, and, eventually, the outer reaches of the universe. These results will help determine how occupational exposure limits to hazardous materials in reduced gravity compare to the occupational exposure limits in normal gravity. Further, the results may impact how NASA engineers design future space equipment and stations (ie, with or without the same materials, and in the same or different amounts to limit exposure).

Specific Objective 1

Our first specific objective was to determine whether human genotoxic agents damage cells and DNA more in altered than in normal gravity. The focus of this objective was to measure the effects of altered gravity on DNA damage caused by exposure to chemicals. We considered the ability of chemicals to induce chromosome damage in normal, hyper-, and microgravity. By treating cells according to the schedule in Table 1, we measured the amount of chromosomal abnormalities produced in metaphase cells after Na₂CrO₄ exposure using the Wise Laboratory’s published methods for chromosome damage (Xie et al., 2004). We measured the amount of DNA double-strand breaks using immunofluorescence of H2A.X foci, as each focus is considered to represent one DNA double-strand break. We also used the Wise Laboratory’s published methods for H2A.X foci formation.

Table 1. Outline of Experiments for Specific Objective 1

Experiment	Purpose	Treatment	Procedure
Chromosome damage	Confirm that chromosome damage is increased by altered gravity	Na ₂ CrO ₄ (0, 5, 10, 20 μM)	<ul style="list-style-type: none"> • Treat cells 1 h before takeoff • Allow cells to incubate in warm environment on plane • Harvest 1 h after landing
DNA double-strand breaks	Determine whether DNA breaks are also increased by altered gravity	Na ₂ CrO ₄ (0, 5, 10, 20 μM)	<ul style="list-style-type: none"> • Treat cells 1 h before takeoff • Allow cells to incubate in warm environment on plane • Harvest 1 h after landing

Cells were treated on the ground and then harvested shortly after landing, as described in Table 1. After the experiments were completed and the cells harvested, the cells were prepared to be sent back to Maine for microscopic analysis in the Wise Laboratory. We are analyzing 100 metaphases per dose, and the results will be expressed as percentage of metaphases with damage and total damage in 100 metaphases. We predict that altered gravity will result in an increase in the amount of DNA damage and the percentage of metaphases with damage. For DNA double-strand breaks, cells were harvested at the cessation of the experiments and preserved for foci formation measurement before they were shipped to the Wise Laboratory for analysis on a confocal microscope. We will analyze 50 cells per dose and the results will be expressed as average number of foci per cell. We predict that altered gravity will increase the level of DNA double-strand breaks.

Specific Objective 2

Our second specific objective was to determine whether the change in the amount of chromosome damage is due to an increase in the cellular uptake of chemicals by facilitated diffusion and phagocytosis in altered gravity. We tested the effects of altered gravity on cellular uptake of chemicals. We measured ion uptake and particle internalization in normal and altered

gravity, and treated cells according to the schedule in Table 2. We then measured the amount of Cr ion inside the cell after a 4-h exposure to Na_2CrO_4 using the Wise Laboratory's published methods for inductively coupled plasma atomic emission spectroscopy (ICP-AES) (Holmes et al., 2005). Cells were treated on the ground and harvested shortly after landing, as described in Table 2. After the experiments were completed, cells were frozen and shipped to the Wise Laboratory. There, cells will be analyzed for uptake using ICP-AES (ion uptake) or transmission electron microscopy. Data will be presented as μM Cr in the intracellular and extracellular environment and percentage of cells with internalized particles. We predict that altered gravity will result increase the uptake of ions, thereby increasing the frequency of DNA and chromosome damage.

Table 2. Outline of Experiments for Specific Objective 2

Experiment	Purpose	Treatment	Procedure
Cr ion uptake	Determine the effects of altered gravity on the uptake of Cr ions to compare with the DNA damage studies in Specific Objective 1	Na_2CrO_4 (0, 5, 10, 20 μM)	<ul style="list-style-type: none"> • Treat cells 1 h before takeoff • Allow cells to incubate in warm environment on plane • Harvest 1 h after landing

Specific Objective 3

Our third specific objective was to determine whether the change in the amount of chromosome damage is due to an inhibition of DNA repair mechanisms by altered gravity. In this objective, we tested the effects of altered gravity on DNA repair mechanisms in an altered gravity environment. We measured DNA double-strand breaks using the immunofluorescence of H2A.X foci, as each focus is considered to represent one DNA double-strand break. We treated cells and allowed for a repair time according to the schedule in Table 3. We then measured the average number of H2A.X foci per cell after Na_2CrO_4 exposure using the Wise Laboratory's published methods for H2A.X foci formation. After the experiments were complete, the cells were harvested and preserved for foci formation measurement before they were shipped to the Wise Laboratory for analysis by confocal microscope. We will analyze 50 cells per dose and the results will be expressed as average number of foci per cell. We predict that altered gravity will inhibit DNA repair mechanisms, resulting in a higher number of DNA double-strand breaks.

Table 3. Outline of Methods of Specific Objective 3

Experiment	Purpose	Treatment	Procedure
DNA repair: 4-h treatment preflight	Determine amount of damage in cells before flight	Na_2CrO_4 (0, 5, 10, 20 μM)	<ul style="list-style-type: none"> • Treat 5 h before takeoff • Harvest 1 h before flight
DNA repair: 4-h treatment preflight + 4-h repair recovery	Determine effects of altered gravity on recovery of DNA damage	Equal treatment/recovery time intervals Na_2CrO_4 (0, 5, 10, 20 μM)	<ul style="list-style-type: none"> • Treat 5 h before takeoff • Add vitamin C 1 h before takeoff • Keep in incubator for flight duration • Harvest 1 h after landing
DNA repair: 4-h treatment preflight + 24-h repair recovery	Determine effects of altered gravity on recovery of DNA damage after 4-h treatment interval over standard recovery interval, beginning on flight	Short treatment time; standard recovery time, beginning in altered gravity Na_2CrO_4 (0, 5, 10, 20 μM)	<ul style="list-style-type: none"> • Treat 5 h before take-off • Add Vitamin C 1 hour before takeoff • Keep in incubator for flight duration • Store in incubator for 22 h • Harvest after 24-h recovery

RESULTS

We do not have completed data from this year's experiments because it takes several weeks (sometimes months) to complete data analysis and we are currently analyzing our data. The results shown in figures 4 and 5 are based on last year's experiments. We anticipate similar results from this year's experiment.

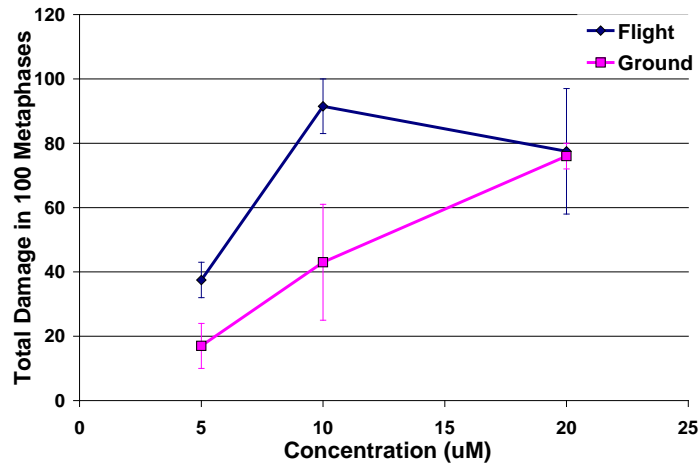


Figure 4. Chromosome damage resulting from Na_2CrO_4 treatments. The data show there is a much higher incidence of chromosome damage in flight than on the ground. For example; at 10 μM , there are 43 chromosome aberrations per 100 metaphases on the ground and 92 in flight.

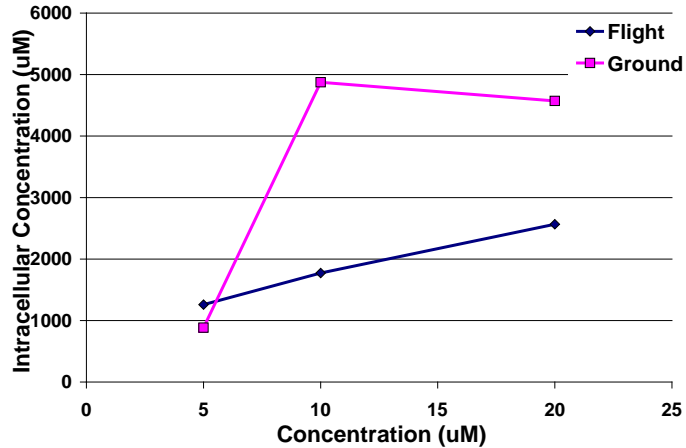


Figure 5. Cr uptake resulting from Na_2CrO_4 treatments at varying concentrations. Unlike what we expected to find, the data show there is a much lower Cr uptake in flight than on the ground. For example: at 10 μM , the uptake is 1,773 μM in flight and 4,874 μM on the ground.

Now, if we take the intracellular Cr concentrations that we found in the uptake experiments and graph them against the total amount of chromosome damage, we can more accurately demonstrate the effects of altered gravity, as shown in figure 6.

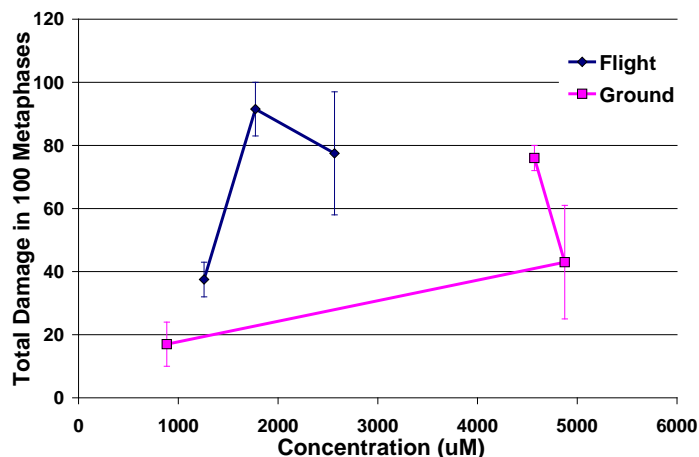


Figure 6. Chromosome damage resulting from the intracellular Cr concentration. The graph illustrates the following: (1) flight increases the rate at which chromosome damage occurs; (2) there is much more damage in flight than on the ground (eg, at 1773 μM , there are approximately 23 aberrations in the ground experiments; in flight, there are 92).

DISCUSSION

Based on the results from our chromosome damage experiments, a combination of hyper- and microgravity causes an increase in the number of chromosomal aberrations induced by Na_2CrO_4 . We used three concentrations of Na_2CrO_4 (5, 10, and 20 μM) and a negative control (0 μM) to consider a dose response. Our results showed that altered gravity dramatically increased chromosome damage inducing two to three times the total amount of damage present in 100 metaphase cells and in the percentage of metaphase cells with damage. Analyzing the data, we observed that the total amount of chromosome damage and the percentage of damaged metaphase cells in altered gravity drops at doses between 10 and 20 μM , which is most likely due to an increase in cell death removing severely damaged cells from the population.

Results from our experiments to determine the effects of altered gravity on cellular uptake of chemicals indicate there is less uptake of chemicals in flight than on the ground. Again, we used three concentrations of Na_2CrO_4 (5, 10, and 20 μM) and a negative control (0 μM). Unlike our hypothesis, our results indicated that altered gravity inhibited a cell's ability to take up Cr(VI) ions. We used ICP-AES to analyze our samples, and found the normal gravity samples had approximately twice the number of Cr ions as the altered gravity samples. We observed a drop between the 10 and 20 μM treatments (similar to what we saw in the chromosome damage experiments), and believe this drop to be a result of altered gravity increasing the occurrence of apoptosis.

Last year's results to determine the effects of hyper- and microgravity on DNA repair mechanisms are incomplete because the antibody needed to analyze these slides failed. During DNA repair, a protein called H2A.X responds by accumulating around damaged DNA strands and initiating the repair process. We detected the H2A.X by adding an antibody that binds only to the protein; this antibody is fluorescent and can be detected using a green light filter under a microscope. We conducted similar experiments at our laboratory to determine how long it would take for DNA repair to occur. After treating cells with 10- μM Na_2CrO_4 for 4 h before co-treating then with vitamin C for 4, 6, and 24 h, we observed approximately half of the foci after a 4-h repair

period. We did the same set of experiments with a 20- μ M treatment, but did not see any repair until after 24 h. Thus, we expect to be able to find some significant results from this year's experiments.

CONCLUSION

Our hypothesis predicted that due to the known morphological alterations cells undergo in zero gravity (Crawford-Young, 2006; Tischler and Morey-Holton, 1993), the altered-gravity environment that astronauts experience will have implications on cellular function, such that chemically induced genotoxicity will be exacerbated. We hypothesized that this effect would result from an increase in cellular uptake of chemicals and/or inhibition of DNA repair mechanisms. After analyzing the results from our chromosome damage experiments, we confirmed our hypothesis that altered gravity exacerbates chemically induced genotoxicity. However, altered gravity does not increase the amount of background damage, which means that flight alone is not genotoxic. Our results indicate that crewmembers exposed to genotoxic chemicals in flight could be at greater risk than expected. We predicted this effect would be a result of the increased cellular uptake of ions, but our data proved our hypothesis incorrect. Instead, we found the cellular uptake of ions to be drastically inhibited. We anticipate the data from this year's experiment to show the same results, and indicate whether the exacerbated genotoxicity is due to inhibited DNA repair mechanisms or some other unknown factor.

REFERENCES

1. Wise SS, Elmore LW, Holt SE, et al. Telomerase-Mediated Lifespan Extension of Human Bronchial Cells Does Not Affect Hexavalent Chromium-Induced Cytotoxicity or Genotoxicity. *Mol Cell Biochem*, 2004;255:103-111.
2. Wise JP Sr, Wise SS, Little JE. The Cytotoxicity and Genotoxicity of Particulate and Soluble Hexavalent Chromium in Human Lung Cells. *Mutat Res*. 2002;517:221-229.
3. Costa M, Klein CB. Toxicity and Carcinogenicity of Chromium Compounds in Humans. *Crit Rev Toxicol*. 2006; 36.2:155-163.
4. Blankenship LJ, Carlisle DL, Wise JP Sr, Orenstein JM, Dye LE III, Patierno SR. Induction of Apoptotic Cell Death by Particulate Lead Chromate: Differential Effects of Vitamins C and E on Genotoxicity and Survival. *Toxicol Appl Pharmacol*. 1997;146:270-280.
5. Xie H, Holmes AL, Wise SS, Gordon N, Wise JP Sr. Lead Chromate-Induced Chromosome Damage Requires Extracellular Dissolution to Liberate Chromium Ions but Does Not Require Particle Internalization or Intracellular Dissolution. *Chem Res Toxicol*. 2004;17.10:1362-1367.
6. Wise SS, Holmes AL, Ketterer ME, et al. Chromium Is the Proximate Clastogenic Species for Lead Chromate-Induced Clastogenicity in Human Bronchial Cells. *Mutat. Res*. 2004;560: 79-89.
7. Xie H, Wise SS, Holmes AL, et al. Carcinogenic Lead Chromate Induces DNA Double-Strand Breaks in Human Lung Cells. *Mutat. Res*. 2005;586(2):160-172.
8. Crawford-Young SJ. Effects of Microgravity on Cell Cytoskeleton and Embryogenesis. *Int J Dev Biol*. 2006;50:183-191.
9. Tischler ME, Morey-Holton E. *Space Life Sciences Research: The Importance of Long-Term Space Experiments*. Washington, DC: NASA Headquarters; 1993; NASA-TM-4502.
10. Holmes AL, Wise SS, Xie H, Gordon N, Thompson WD, Wise JP Sr. Lead ions do not cause human lung cells to escape chromate-induced cytotoxicity. *Toxicol Appl Pharmacol*. 2005;203:167-176.

PHOTOGRAPHS

JSC2009E135194 to JSC2009E135197

JSC2009E137325

JSC2009E137316

JSC2009E137339

JSC2009E137558 to JSC2009E137559

JSC2009E137577 to JSC2009E137578

JSC2009E137598 to JSC2009E137600

JSC2009E137631 to JSC2009E137649

VIDEO

- Zero G flight week 6/5 – 6/12, 2009 Master: 743649

Videos are available from Imagery and Publications Office (GS4), NASA Johnson Space Center (JSC).

CONTACT INFORMATION

John P. Wise, Jr.

john.p.wise@maine.edu

Dr. John P. Wise, Sr.

john.wise@maine.edu

Dr. Michael Mason

mmason@umche.maine.edu

TITLE

High-Accuracy Eye-Movement Monitor

FLIGHT DATES

August 11–12, 2009

PRINCIPAL INVESTIGATOR

Mark Shelhamer, Johns Hopkins University, School of Medicine, Baltimore, MD

COINVESTIGATORS

Kara Beaton, Johns Hopkins University, School of Medicine, Baltimore, MD

Aaron Wong, Johns Hopkins University, School of Medicine, Baltimore, MD

Dale Roberts, Johns Hopkins University, School of Medicine, Baltimore, MD

Michael Schubert, Johns Hopkins University, School of Medicine, Baltimore, MD



GOAL AND OBJECTIVES

To validate, in a realistic space analog environment, the performance of a device for accurate high-resolution measurements of eye movements during head and body motions. This device can aid future research programs into human sensorimotor adaptation to spaceflight.

INTRODUCTION

The control of eye movements represents one of the most basic and fundamental motor control systems of the human brain, combining information from both low-level motion transducers in the inner ear (the vestibular system) and high-level visual information. The measurement of eye movements thus can provide important information on many forms of sensorimotor processing. Long-duration spaceflight has been shown to adversely affect many aspects of sensorimotor function, which can have serious implications on manually controlled tasks and piloting performance, especially during maneuvers involving transitions in G-level. Therefore, the ability to measure eye movements with high spatial and temporal precision, during natural head and body motions, can be a valuable aid to monitoring these effects.

METHODS AND MATERIALS

The technology tested in this project is an improved version of the standard scleral search-coil method, the current “gold standard” for measurement of eye movements. An annular contact lens that sits on the eye contains a passive resonant coil/capacitor circuit. A transmitter coil and small (2.5 cm) cubes of receiver coils are placed near the eye on a headset and connected to associated electronics. The transmitter coils are pulsed to generate bursts of magnetic field energy that stimulate the resonant coil in the contact lens. After each burst of pulses, the receiver coils act as directional antennae, transducing the electromagnetic field radiated by the resonant scleral coils. A dedicated processing unit then amplifies, digitizes, and determines the magnitudes of the received waveforms, which depend on the orientation of the resonant coils on the eye relative to the set of receiver coils. By using this magnitude information, we can determine the orientation of the coil (and eye). The contact lens assembly is based on a commercial lens in widespread use that we modified by attaching a resonating capacitor (figure 1).

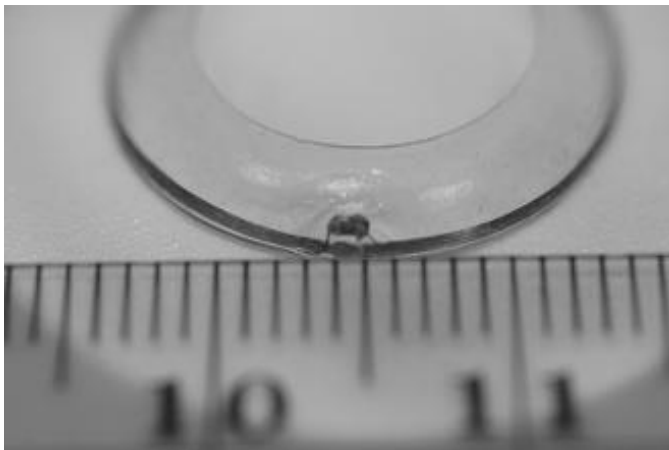


Figure 1. Wireless coil.

For this study an engineering evaluation of this device is performed in parabolic flight during which a test subject, wearing the device, makes head and body movements. A rate-sensor/accelerometer package on the headset measures head movements. Testing in parabolic flight is critical when validating the device for later use in spaceflight (and further parabolic-flight experiments) to assess any shifting of the headset on the head and any changes in overall comfort and effectiveness in different gravity levels.

Information on position as well as orientation (with respect to the headset) of an eye coil is obtained using multiple receiver coils (figure 2); this allows measurement of headset motion relative to the head by taping an “eye coil” to the head as a reference.

RESULTS

At the time of the flights, we did not have the JSC’s Committee for the Protection of Human Subjects (CPHS) approval to place a contact lens on the subject’s eye while the subject was in flight. We are working to resolve this problem, which we expect to accomplish in the near future (the Johns Hopkins Institutional Review Board [IRB] has approved this project for use in parabolic flight). Therefore, we evaluated several engineering aspects of the device besides its ability to measure eye movements. These aspects are: robustness and ease of use of the hardware and software, signal quality and noise level, comfort of the head unit, and slip of the head unit during movements at different gravity levels. This engineering evaluation consisted of having one of the investigators wear the head unit while making natural movements. A rate-sensor/accelerometer package on the head unit measured head movements, as did, for comparison, a similar set of sensors on a biteboard.

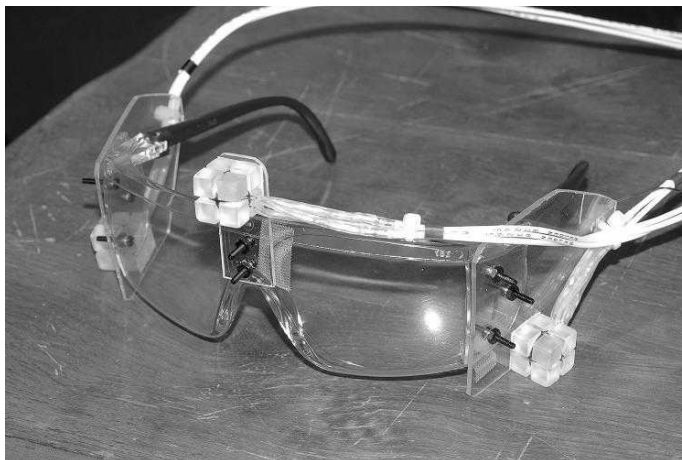


Figure 2. Head-mounted assembly, showing multiple sets of receiver coils.

Testing revealed satisfactory usability of hardware and software, although work remains to be done on a real-time graphical display that will show signal and noise levels. Signal quality and head slip appear adequate, although we have not yet processed these data fully. The head unit was found to be prone to wiring damage during stowage. This damage, which was found before the first flight, was fixed on site although it recurred during the second flight, thus limiting the overall data return. Subject comfort (and, to some extent, head-unit stability) was limited by the cabling from the head unit to the electronics package. This umbilical was almost 2 cm in diameter and not very flexible, which required that it be clamped to the subject’s flight suit in several places for strain relief, thereby limiting comfort and freedom of movement.

DISCUSSION/CONCLUSION

Development of this device continues, with special attention paid to the shortcomings revealed during the flights, as noted above. Specifically, a user-friendly software interface will be developed; more robust electrical wiring will be implemented; and smaller, more flexible umbilical wiring will be considered. We anticipate that after making these changes, we will obtain CPHS approval for actual eye-movement recording, integrate the device with a set of visual stimuli for sensorimotor testing, and test this integrated and improved package during flights in the 2010 Facilitated Access to Space Environment for Technology Development and Training (FAST) program.

REFERENCES

1. Roberts D, Shelhamer M, Wong A. A new “wireless” search-coil system. In: *Proceedings of the Eye Tracking Research & Applications Symposium, Savannah, Georgia, 26-28 March 2008*;197-204.
2. Robinson DA. A method of measuring eye movement using a scleral search coil in a magnetic field. *IEEE Trans Biomed Eng.* 1963;10:137-145.

VIDEO

- Zero G flight week 8/11 – 8/14, 2009 Master/TSR: 103823

Videos are available from Imagery and Publications Office (GS4), NASA JSC.

ACKNOWLEDGEMENT

This work was supported by the NASA FAST Program.

CONTACT INFORMATION

Mark Shelhamer
Johns Hopkins University, School of Medicine
210 Pathology Bldg.
600 N. Wolfe St.
Baltimore, MD 21287
mjs@dizzy.med.jhu.edu
410-614-6302

TITLE

FASTRACK Program – Antimicrobial Polymers Project

FLIGHT DATES

August 10–14, 2009

PRINCIPAL INVESTIGATORS

Luke Roberson, Kennedy Space Center, FL

Mike Roberts, Dynamac Corporation, Kennedy Space Center, FL

David Makufka, Kennedy Space Center, FL

Amy Hitabel, AP Solutions, Glenn Research Center, OH



GOALS

To develop test methods and generate microbiological data to be used in the verification of the antimicrobial efficacy of materials and biocides in wetted systems.

INTRODUCTION/BACKGROUND

The vision for human space exploration requires integrated technologies to collect, store, recycle, and disinfect water for use and reuse in environmental control and life support systems (ECLSS) for spacecraft missions. In addition to maintaining water quality for crew use, these systems must minimize mass, power, and resupply requirements. Microbial control technologies currently employed by NASA for spacecraft potable water systems require the use of a residual chemical biocide such as silver (Ag) or iodine and one or more physical disinfection devices to reduce the microbial burden. None of these chemical biocides are completely effective against all microorganisms, however, and all have limitations for long-term use because they do not provide an absolute barrier to microbial growth, become inactive over time, require repeated additions, and/ or pose risks to human health with prolonged use. An antimicrobial solution is needed that improves microbial control and provides a safe, long-lasting, and non-leaching antimicrobial surface useful for long-duration spaceflight applications.

A recent approach to resisting surface microbial colonization is to modify the surface roughness to emulate naturally occurring anti-fouling surfaces. Sharklet™, developed by Sharklet Technologies, Inc. (Alachua, FL), is a highly specific, micron-scale surface pattern inspired by the surface roughness associated with the skin of sharks. The Sharklet™ micro-pattern may be engineered into new or existing material surfaces to inhibit microorganism growth (Schumacher, 2007A; Schumacher 2007B; Carman, 2006) and delay the formation of bacterial biofilm (Chung, 2007). As the surface micro-patterning technique adds no new material to the surface, the surface maintains its original chemistry and material properties. This purely physical approach to inhibiting biofilm formation does not rely on the incorporation of antimicrobial agents, thus sidestepping the problems associated with reduced antimicrobial activity and health risks.

The development of antimicrobial coating methods stems from the commonly held belief that bioadhesion is primarily influenced by the chemical composition and activity of the surface. While this is an important factor, the influence of surface topography can be a dominant variable in predicting bioadhesion. It has long been known that surface roughness affects wettability, which has motivated the study of the physical modification of a material surface with topography as a means to control bioadhesion (Schmidt, 1991; den Braber, 1996; den Braber, 1998; van Kooten, 1998; van Kooten, 1999). While surface topography has been explored in a trial-and-error fashion for randomly roughened surfaces and some ordered topographies, only recently has the interrelationship of topography, wettability, and bioadhesion been investigated (Carman, 2006). These studies have indicated that engineered topographies—particularly geometries of ordered features designed with unique roughness properties—do elicit specific, predictable biological responses. This strategy for controlling bioadhesion represents a paradigm shift in the current methods using antimicrobial agents. Applying a surface topography instead of antimicrobial agents relies on controllably changing the surface energy so as to affect bioadhesion.

Polymer surface micro-patterning is an area of research and development that has expanded significantly in both the private sector and academia. Several methods for accomplishing this

exist, and all methods rely on the use of a master or mold and are derived by altering parameters such as heat, ultraviolet (UV) exposure, and pressure. They include photolithography, soft lithography (including micro-contact printing, replica molding, micro-transfer molding, micromolding in capillaries, and solvent-assisted micromolding) (Xia, 1998; del Campo, 2008; Gates, 2005), soft molding (Kim, 2001; Choi, 2004), polymer casting (Gates, 2005), hot embossing (Chang, 2003), UV imprint lithography (Bailey, 2002; Cheng, 2008; Haatainen, 2008; Kim, 2003; and Rudschuck, 2000), ion beam proximity patterning, and focused ion beam writing. These methods have been widely used and perfected for replicating micron-scale features into flat substrates; several demonstrate feasibility for large-area printing—a necessity for manufacturing scale production (Suho, 2006; Suho, 2007; Kunnavakkam, 2003; Makela, 2008; Gates, 2005; and Xia, 1998). A few of these methods (eg, hot embossing and micro-contact printing) have been studied for application to curved surface patterning (Chang, 2005; Cheng, 2006; Choi, 2004; Makela, 2008; Tanaka, 2007; and Paul, 2003).

An engineered roughness index (ERI) model has been previously described (Schumacher, 2007A) for predicting the biological response to micro-patterns. The model predicts the wetting and de-wetting potential of a particular surface roughness and can be used to develop patterns with optimized roughness (Schumacher, 2008; Schumacher, 2007B; Carman, 2006). The dimensionless ratio allows for characterization of engineered roughness that expands on traditional definitions of roughness for topography:

$$ERI = (r * df) / f_D$$

The ERI is a function of three variables associated with the geometry, size, and spatial arrangement of the topographical features: Wenzel roughness factor (r), depressed surface fraction (f_D), and degrees of freedom (df). The ERI is based on the hypothesis that increased tortuosity, or the dimensionality and orientation of the spacing between features in the surface topography, renders the surface less favorable for organism adhesion. Larger ERI values imply reduced settlement of biological microorganisms (Schumacher, 2007A).

Aspect ratio, including feature height and feature width, can be adjusted to improve ERI values; for example, increased feature height increases surface area, leading to a higher ERI. A variation of the Sharklet[™] micro-pattern with the same spatial arrangement of features but with depressed recesses instead of protruding features, called inverse Sharklet[™] (ISK), would decrease f_D , resulting in an increased ERI.

In combination with non-leaching antimicrobial additives, Sharklet[™] would provide persistent, long-term biological protection to polymeric and metal surfaces against a broad spectrum of bacteria, fungi, and protozoa without need for biocide re-application. To verify that the microbial control technology is effective in maintaining high purity water requirements from vehicle loading through mission operations, antimicrobial materials for use in spacecraft ECLSS were first evaluated for the impact of variable gravity environments on cellular adhesion. In this study, the ISK and Sharklet[™] micro-patterns were evaluated in different material compositions for the ability to resist colonization in lunar gravity and microgravity conditions.

METHODS AND MATERIALS

Pre-travel Procedure

Sharklet Technologies, Inc. provided NASA with 30 coupons for ground testing and a further 110 coupons for reduced-gravity flight operations, as described below. They provided 15 PDMS (polydimethylsiloxane) elastomer coupons with the Sharklet™ pattern, 15 PDMS coupons with ISK pattern, and 15 PDMS coupons without a pattern. NASA personnel performed change data capture (CDC) bioreactor testing on the Sharklet™ PDMS coupons following methods defined in ASTM (American Society for Testing and Materials) E 2562-07, as previously conducted at KSC, to compare the extent of biofilm formation on new materials with that previously observed. Additionally, Sharklet Technologies, Inc. supplied ISK-patterned PDMS coupons for NASA to apply a peptide coating to a subset of materials to include in CDC reactor testing. NASA also included additional material coupons from the Air Force Research Laboratory (AFRL) (Wright-Patterson Air Force Base, Dayton, OH) for CDC reactor testing.

NASA personnel tested a subset of material coupons in the BRIC (biological research in a canister) flight hardware containing either a standard Petri dish fixation unit (SPDFU) or a modified Petri dish fixation unit (MPDFU) for verification of ground- and flight-test procedures to determine antimicrobial activity within the duration of reduced-gravity parabolic flight operations.

Flight Hardware

BRIC-LED (biological research in a canister light-emitting diode) flight hardware is an anodized-aluminum container capable of providing illumination and fixation capability for the cultivation of small biological specimens in a complement set of flight hardware, the Petri dish fixation unit (PDFU) (figure 1). Each BRIC-LED canister can accommodate as many as six PDFUs. Each PDFU contains a single 60 × 15-mm Petri dish and a fluid reservoir for on-orbit activation and/or chemical fixation of biological samples in the PDFU. The SPDFU contains a single-chamber reservoir for the addition of one fluid during flight operations. The MPDFU contains a dual-chamber reservoir for the addition of two fluids during flight operations.



A



B

Figure 1. Flight hardware: A. The BRIC and B. The PDFU.

Pre-flight Procedure at KSC

Sharklet Technologies, Inc. provided NASA with 110 polycarbonate (PC) coupons without pattern, 90 PC coupons with the ISK pattern, 110 PDMS coupons without pattern, and 90 PDMS coupons with both Sharklet™ and ISK patterns. In addition, Sharklet Technologies, Inc. supplied low-density polyethylene (PE) coupons with and without the ISK pattern. NASA provided 80

stainless-steel (SS) and 80 titanium (Ti) coupons. All coupons were 12 mm in diameter and had an adhesive backing for mounting into BRIC PDFUs.

NASA personnel treated all coupons by ethylene oxide (EtO) sterilization for payload integration with flight hardware treated by autoclave sterilization and assembled by the Flight Payloads Group (Bionetics Corporation, Yorktown, VA) at KSC per procedures contained in the Antimicrobial Polymer Project Work Authorization Document (LSSC-WAD-AMPP [launch services support contract-work authorization document-Advanced Materials Processing Program]). Sterile test coupons and either ionic Ag biocide ($400 \mu\text{g}\cdot\text{L}^{-1}$ AgF) (Sigma-Aldrich, St. Louis, MO) or cell fixative (1% formalin, Sigma Aldrich) were aseptically loaded into the flight hardware in a laminar flow bench or biological safety cabinet (BSC) for shipment by government van in sealed flight hardware shipping containers to the JSC Advanced Water Recovery System Development Facility (AWRSDF) in Building 7B. An agar streak plate of the test microorganism, *Pseudomonas aeruginosa* strain ERC1 (ATCC 700888), was prepared at KSC for shipment to JSC in a separate container. The bacterial inoculum for reduced-gravity testing was prepared as a broth culture in BBL™ Trypticase™ Soy Broth (TSB) (BD, Franklin Lakes, NJ) from the agar streak plate ≥ 12 h before flight each flight day and loaded into the flight hardware at JSC in a BSC.

In total across two flight days, 70 treatments—comprised of seven identical coupons affixed to the bottom of a 60-mm Petri dish housed in a PDFU mounted inside of each BRIC (ie, seven coupons per PDFU, six PDFUs per BRIC, six BRICs per flight day)—were performed, except as noted. After each flight day, MPDFUs were removed from the BRIC units and stored at 4°C for return to KSC. SPDFUs were de-integrated from their BRIC and the coupons were aseptically transferred from each Petri dish to sterile containers for analysis at JSC or KSC. At JSC on each flight day, two coupons were sampled for heterotrophic plate count (HPC) on R2 agar (BD, Franklin Lakes, NJ), two coupons for LIVE/DEAD® BacLight™ (Invitrogen, Carlsbad, CA) direct count live/dead (L/D), and one coupon for ATP (LuminUltra Technologies Ltd., Fredericton, New Brunswick, Canada) quantification. For coupons from each SPDFU to be sampled at KSC, one coupon was fixed in 1% formalin using the acridine orange direct count (AODC) (Sigma Aldrich) technique and one coupon was suspended in sterile phosphate buffered saline (PBS) (Sigma Aldrich) for scanning electron microscopy (SEM). In addition to coupon samples, bulk fluid from each PDFU was assayed at JSC by HPC, L/D, AODC, and ATP.

The HPC test, also called the total count or plate count, provided an estimate of the total number of bacteria that developed into colonies during a period of incubation on a nutrient-rich agar (eg, R2A) in a sample. This test, which can detect a broad group of bacteria including non-pathogens, pathogens, and opportunistic pathogens, often does not accurately sample all of the bacteria in the water sample examined. For example, bacterial biofilms, injured bacteria, and/or viable but non-culturable bacteria may not form colonies on the selected nutrient medium. In some cases, samples required serial dilution for enumeration. The results were averaged and the standard deviation was calculated for both the HPC and the AODC sample data. For direct counts of cells the formalin-fixed water samples were sonicated, diluted into 0.2- μm filtered deionized water, stained with acridine orange (AO), and filtered onto 25-mm (dia.), 0.2- μm black polycarbonate filters for enumeration on an Axioskop 2 epi-fluorescent microscope (Carl Zeiss Micromalging, Inc., Thornwood, NY) at 1,000 \times magnification (Bloem, 1995; Hobbie et al., 1977). The LIVE/DEAD® BacLight

bacterial viability kit (Invitrogen) had previously been used to determine the percentage of viable organisms found in a urine sample (Boulos et al., 1999; Gregori et al., 2001). Viability, as determined by BacLight™ assay and that equates with cells that have intact cell membranes, tends to overestimate living cells in most environmental matrices.

Adenosine Triphosphate Procedure

Bulk Fluid Adenosine Triphosphate Procedure Assay Protocol

The following are instructions for the Quench-Gone Aqueous (QGA™) test kit:

- Remove the plunger from a 60-mL syringe (provided by manufacturer)
- Add a filter (provided by manufacturer) to the 60-mL syringe
- Vortex each sample for 5 s
- Pipette 3 mL of sample with a 5-mL serological pipette into the syringe with filter
- Replace the plunger
- Slowly filter the sample into a 1-L beaker (waste receptacle)
 - Filter all fluid through, but allow the filter to remain wet
- Detach the filter and remove the plunger
- Reattach the filter to the syringe
- Add 1 mL of UltraLyse 7 to the barrel
- Collect the extract fluid in a dilution tube until the filter is dry
- Add 9 mL of UltraLute to the extract with a 10-mL serological pipette (10 mL total volume)
- Cap and invert three times to mix
- Pipette 100 µL of diluted extract into a well of the black-and-white Isoplate
- For the control well, add 100 µL of UltraCheck 1 (two drops)
- Add 100 µL of room-temperature Luminase (two drops) to all wells containing samples
- Swirl gently five times to mix
- Load into the PerkinElmer VICTOR™ X2 plate reader (PerkinElmer, Covina, CA) and run luminescence assay (×3)

Modified Coupon Adenosine Triphosphate Procedure Assay Protocol

The following are instructions for the modified coupon ATP assay protocol:

- Place a sample in a 15-mL extraction tube containing 1 mL of UltraLyse 7
 - Ensure the coupon is completely immersed
- Cap and vortex for 5 s
- Incubate sample for 5 min at room temperature
- Transfer the contents of the extraction tube to a dilution tube containing the UltraLute/resin mixture
- Cap and invert three times to mix
- Pipette 100 µL of diluted extract into a well of the black-and-white Isoplate
- For the control well, add 100 µL of UltraCheck 1 (two drops)
- Add 100 µL of room-temperature Luminase XL (two drops) to all wells containing samples
- Swirl gently five times to mix
- Load into the PerkinElmer VICTOR™ X2 plate reader and run luminescence assay (×3)

Microgravity Flight (Reduced-gravity Flight Day 1 – 6 BRICs)

BRIC A – C: 17 MPDFUs containing an inoculum and 400 $\mu\text{g L}^{-1}$ AgF (silver fluoride) biocide

BRIC A: 6 control materials (PC SM [smooth], PE SM, PDMS SM, SS, Ti, and PET [polyethylene terephthalate]/Ag)

BRIC B: 4 Sharklet™ patterned materials (PDMS ISK, PDMS SK, PC ISK, PE ISK)
2 AFRL POSS [polyhedral oligomeric silsesquioxanes] samples (*PC/FD₈T₈, *PC/[NMe₄]⁺FD₈T₈)
*3 coupons per PDFU

BRIC C: 5 Peptide (PC SM P [pilin peptide], PC ISK P, SS P, Ti P, and PET/Ag P)

BRIC D – F: 18 SPDFUs containing only inoculum

BRIC D: PC SM, PC SM P, PC ISK, PC ISK P, PE SM, PE ISK

BRIC E: PDMS SM, PDMS SK, PDMS ISK, SS, SS P, PET/Ag

BRIC F: Ti, Ti P, **PC/AFRL, **PC/FD₈T₈, **PC/[NMe₄]⁺FD₈T₈, **PC/Me₄NF
**4 coupons per PDFU for microgravity flight; **3 coupons per PDFU for lunar-G flight

Lunar-gravity Flight (Reduced-gravity Flight Day 3 – 6 BRICs)

BRIC a / BRIC b / BRIC c

17 MPDFUs containing inoculum and formalin with the same material distribution as in the microgravity flight

BRIC d / BRIC e / BRIC f

18 SPDFUs containing inoculum with the same material distribution as in the microgravity flight.

Table 1 provides the active mean surface area by coupon material type, and figure 2 depicts the BRIC test plan coupon arrangement for both microgravity and lunar gravity experiments.

Table 1. Active Mean Surface Area by Coupon Material Type

Material	Mean Coupon Diameter (mm)	Mean Coupon Thickness (mm)	Mean Surface Area (mm ²)
PC ISK	12	0.1778	119.80
PC SM	12	0.1778	119.80
PC/control	12.7	1.4986	186.47
PC/treatments	12.7	1.7272	195.59
PDMS ISK/SK	12	0.0762	115.97
PDMS SM	12	0.1016	116.93
PE ISK	12	0.1016	116.93
PE SM	12	0.3048	124.59
PET/Ag	12 square	0.0762	147.66
SS	12.7	3.8608	280.72
Ti	12.7	3.6322	271.60

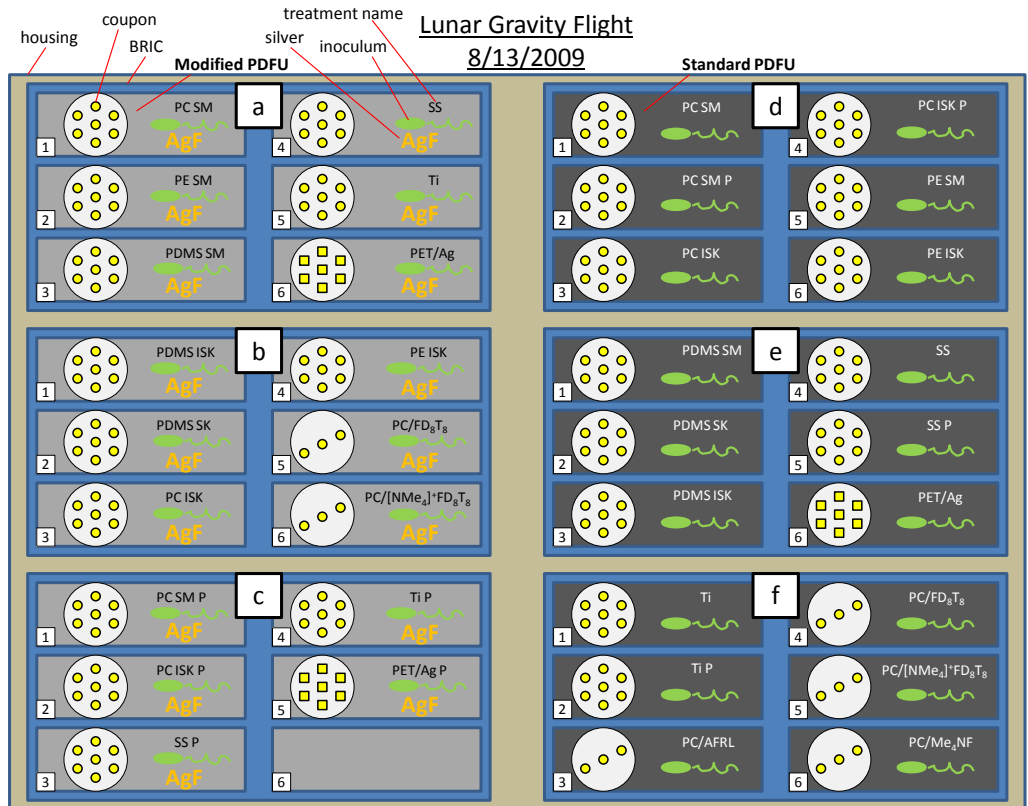
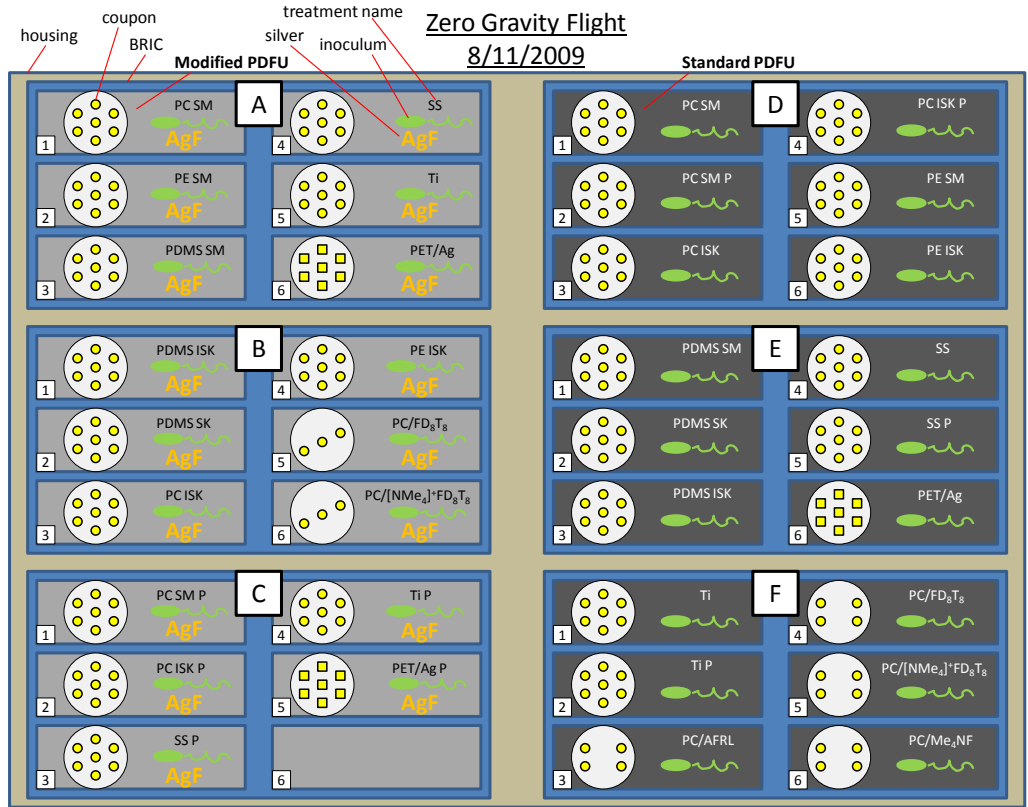


Figure 2. BRIC test plan coupon arrangement for microgravity (top) and lunar-gravity (bottom) experiments.

Preflight Procedure at Johnson Space Center

KSC ground support personnel loaded the PDFU fixation reservoirs at JSC (AWRSDF, Building 7B) with an inoculum on the morning of each flight day containing the test microorganism *P. aeruginosa* strain ERC1 (ATCC 700888) at a cell density of approximately $1E5$ CFU•mL⁻¹ (ie, 100,000 cells/mL). Each SPDFU had a single fixation reservoir with a fill volume of approximately 13 to 14 mL while the MPDFU had two fixation reservoirs, each with a fill volume of approximately 8 to 10 mL. The second fixation reservoir in each MPDFU was filled to capacity (~8 to 10 mL) with either an AgF ionic biocide solution ($400 \mu\text{g}\cdot\text{L}^{-1}$ AgF for the microgravity flight) or 1% formalin fixative (for the lunar-gravity flight) during hardware integration and assembly at KSC as outlined above. BRICs were loaded into foam inserts in a tray at JSC for transport to nearby Ellington Field and integration into a Shuttle middeck locker for attachment to the plane frame with straps for reduced-gravity flight operations, as described in the antimicrobial materials for microgravity environments test equipment data package (AMME-TEDP-RevA).

In-flight Procedure

Microgravity

Before the first parabola was executed, all BRICs (A-F) were manually engaged, thereby exposing the coupons to the microbial inoculum containing [1E5] challenge bacteria in 10% TSB. The samples remained in the inoculum throughout the duration of the reduced-gravity flight. At the end of the last parabola, each BRIC unit containing an MPDFU with Ag biocide solution was engaged again to inject the fluid at the end of the last parabola.

Lunar Gravity

Before the first parabola was executed, all BRICs (a-f) were manually engaged, thereby exposing the coupons to the microbial inoculum containing [1E5] challenge bacteria in 10% TSB. The samples remained in the inoculum throughout the duration of the reduced-gravity flight. At the end of the last parabola, each BRIC unit containing an MPDFU with 1% formalin fixative was engaged again to inject the fluid at the end of the last parabola.

Post-flight Procedure

After each flight day BRICs containing MPDFUs were stored, as is, in coolers with ice packs for return shipment to KSC by ground transport. All MPDFUs were de-integrated from BRICs and processed at KSC for sample analysis to quantify antimicrobial efficacy and cell attachment. BRICs containing SPDFUs were de-integrated from the BRIC units and processed at JSC in the Building 7B. AWRSDF for sample analysis to quantify antimicrobial efficacy and cell attachment. All de-integrated and integrated BRIC and PDFU hardware was packed for return shipment to KSC in accordance with the antimicrobial polymer project work authorization document (LSSC-WAD-AMPP) and under the supervision of flight quality assurance.

A series of treatments similar to the reduced-gravity testing was performed as a ground control at KSC after completion of the micro and lunar parabolic flight experiments.

RESULTS/DISCUSSION

The duration between inoculation and harvest of the SPDFUs was approximately 4.5 h. The duration between fixation and harvest of the MPDFUs was 1 week. HPC results of the bulk fluid samples indicated that experiment and flight hardware performance was nominal (figure 3). The

microgravity flight had an increase of $\text{Log}_{10} \text{CFU/mL} = 0.33$; the lunar gravity flight had an increase of $\text{Log}_{10} \text{CFU/mL} = 0.38$; and the ground testing had an increase of $\text{Log}_{10} \text{CFU/mL} = 0.41$. The HPC results of the bulk fluid samples indicated that variability between PDFUs was minimal for both the flight and the ground experiments (figure 4). HPC data for bulk fluid and coupon samples were unobtainable from MPDFUs after fixation with either 400 ppb ionic Ag or 1% formalin.

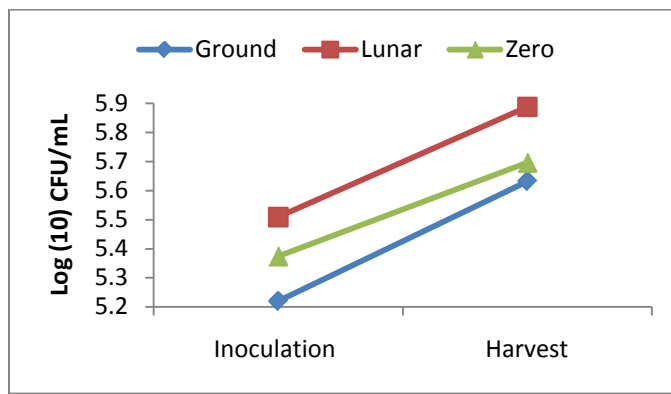


Figure 3. HPC comparison between experiments indicating growth throughout the duration of experiment.

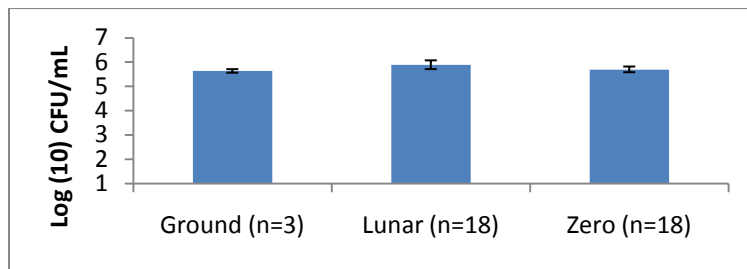


Figure 4. HPC comparison between experiments indicating variation between bulk fluid samples at the time of harvest.

Microscopy data supported the results found from the plate counts for the bulk fluid samples, demonstrating minimal variability between flight experiments. However, the AO and L/D counts were below the limit of detection for coupons recovered for both microgravity and lunar gravity conditions from the MPDFUs and the SPDFUs. During the BacLight™ L/D assay, it was found that 88% to 92% of the cells found in the bulk fluid samples were alive; this result was optimal. The L/D total counts were similar to those found during HPC analysis (figure 5). L/D data for bulk fluid samples was unobtainable from MPDFUs after fixation with either 400-ppb ionic Ag or 1% formalin. Although there were slight variations between the AO samples based on fixation method, these variations were not statistically significant (figure 6). No cells were observed on coupon surfaces during environmental scanning electron microscopy (ESEM).

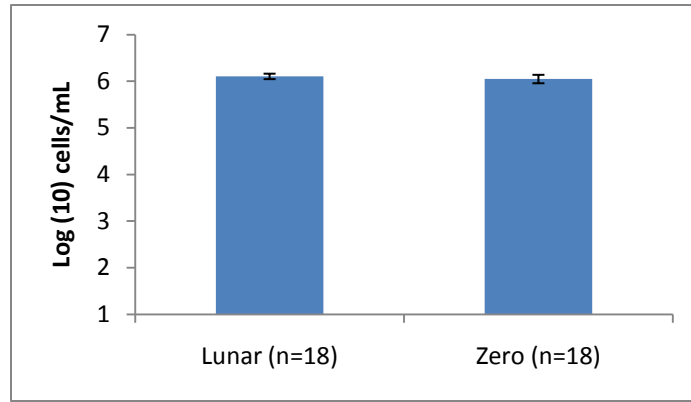


Figure 5. L/D comparison between flights indicating variation in bulk fluid samples.

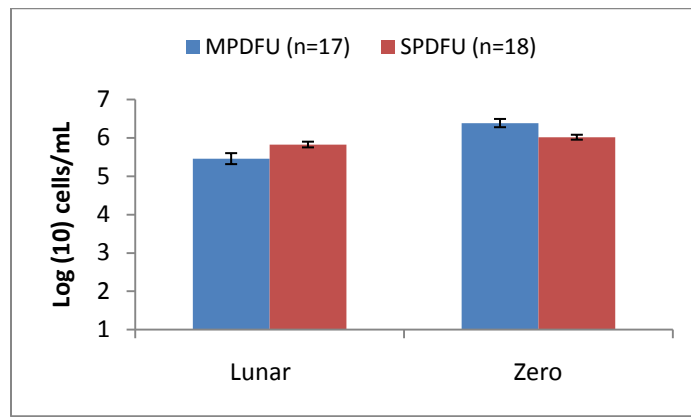


Figure 6. AO comparison between flights indicating variation in bulk fluid based on fixation type.

A standard curve was generated using the LuminUltra™ QGA™ test kit with the *P. aeruginosa* strain ERC1 (ATCC 700888) at a high range of cellular density (figure 7) and a low range of cellular density (figure 8); both ranges showed a positive correlation between the number of cells and the amount of ATP/mL of sample. Cellular concentrations were verified by optical density, AO direct counts, and HPCs. ATP analysis of the bulk fluid samples showed that after 1 week, the microgravity flight produced a 1.6 log reduction after Ag fixation while the lunar gravity flight produced a 2.3 log reduction after formalin fixation. This pattern was repeated to a lesser degree during ground testing in which there was approximately a 1 log reduction in adenosine triphosphate (ATP)/mL with 1% formalin fixation and a > 0.5 log reduction with 400 ppb ionic Ag fixation (figure 9). These results indicate that the formalin has an increased negative impact on cellular metabolism over the Ag.

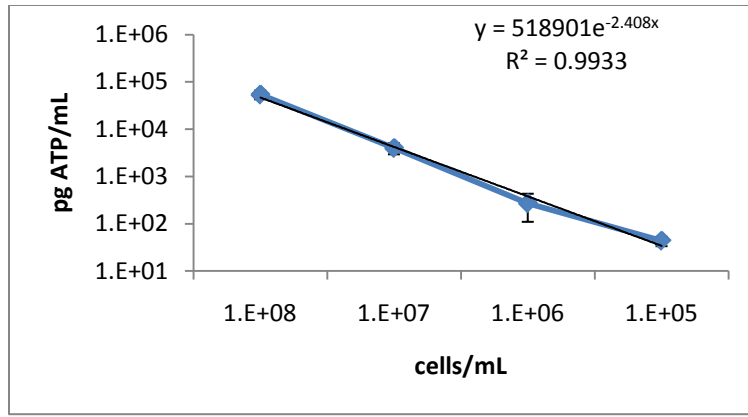


Figure 7. High ATP standard curve (n=9).

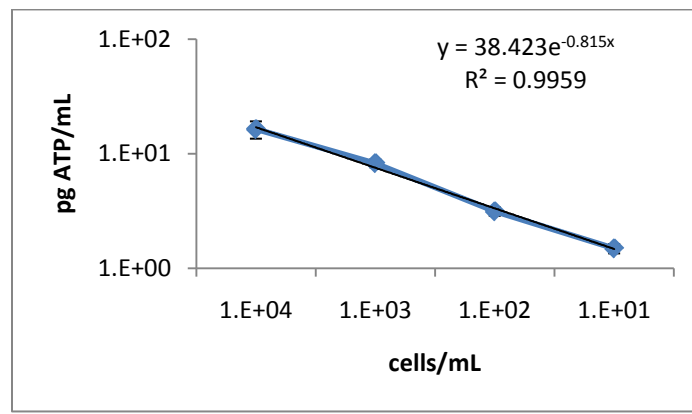


Figure 8. Low ATP standard curve (n=9).

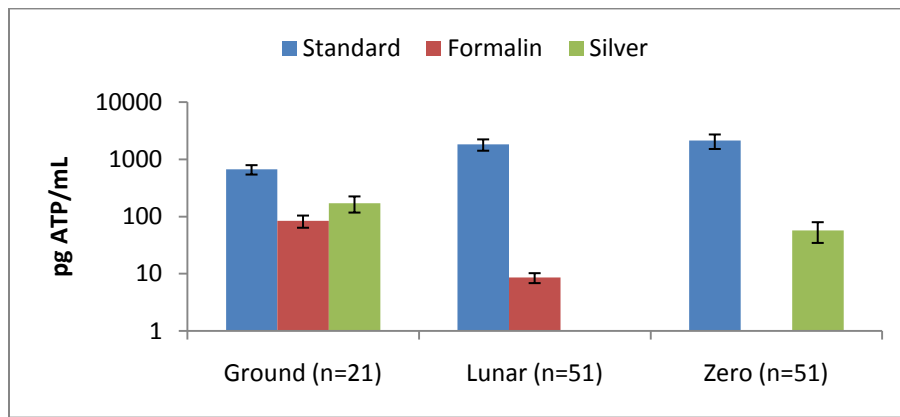


Figure 9. Bulk fluid ATP results.

The previously established benchmark for healthy cells exposed to terrestrial gravity is *Escherichia coli* pg ATP/cell $\approx 1.00E-03$ (Crombrugge and Waes, 1991). This shows that the amount of ATP in the *P. aeruginosa* cells during ground testing resembled the metabolic state of the benchmark samples. More ATP/cell was in those samples experiencing short-duration microgravity exposure than in those during ground testing (Table 2). This effect was previously seen in a study with plants in which cells exposed to short-term microgravity experienced an increased metabolic rate and then, after long-term exposure to microgravity, went into a relaxed

metabolic state lower than even experienced in terrestrial gravity (Hampp et al., 1997). In the cells that were not exposed to a fixative, there appeared to be more ATP/cell in the lunar gravity flight samples than in those that experienced microgravity. After fixation in the MPDFUs for 1 week with either ionic Ag or formalin, there was a 2 log reduction in pg ATP/cell; however, during ground testing this effect was a 1 log reduction in pg ATP/cell.

Table 2. Bulk Fluid pg ATP/Cell Results

	Without fixative	1% Formalin	400 ppb Silver
Ground (n=21)	1.10E-03 ± 3.81E-04	1.38E-04 ± 3.31E-05	2.81E-04 ± 8.83E-05
Lunar (n=51)	2.70E-03 ± 6.05E-04	2.82E-05 ± 5.57E-06	N/A
Micro (n=51)	2.02E-03 ± 5.75E-04	N/A	2.30E-05 ± 9.07E-06

The HPC of the PDMS SK and ISK over the SM decreased in both the lunar and the microgravity flight coupon samples (figures 9 and 10). This effect was more pronounced in the lunar-gravity flight samples (< 1 log reduction). There was a decrease in the HPC of the Ag-coated PET samples over the controls in both the lunar-gravity and the microgravity samples. This effect was more pronounced in the microgravity flight samples (~1 log reduction). During initial coupon ATP testing, the recommended protocol of using a QuenchGone21 wastewater (QG21W) extraction tube with 2 mL of UltraLyse and then adding the sample to a QG21W dilution tube with 8 mL of UltraLute was below the limit of detection for the luminescence assay. The protocol was thus modified to use 1 mL of UltraLyse and 1 mL of UltraLute to lower the dilution factor and produce a response above background due to the low number of cells on the coupons as verified by HPCs. However, this could have made the reaction too alkaline, which could cause inhibition of the Luminase and produce a less-specific reaction.

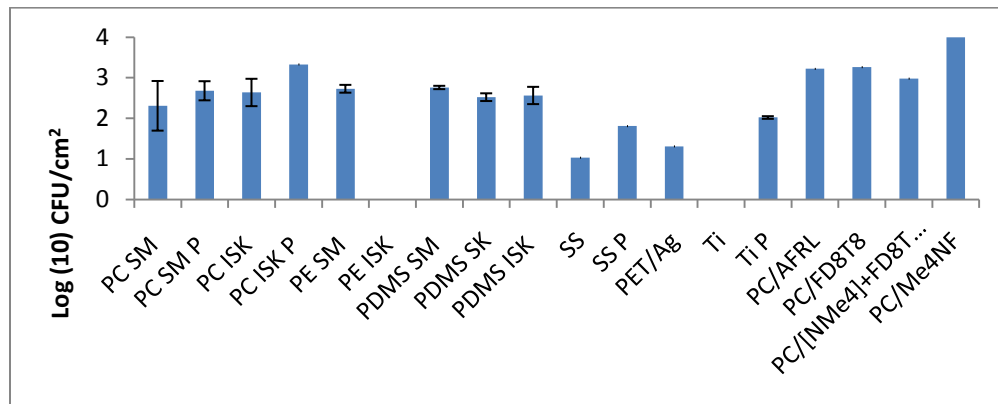


Figure 10. HPC comparison between coupons during the microgravity parabolic flight (n=2).

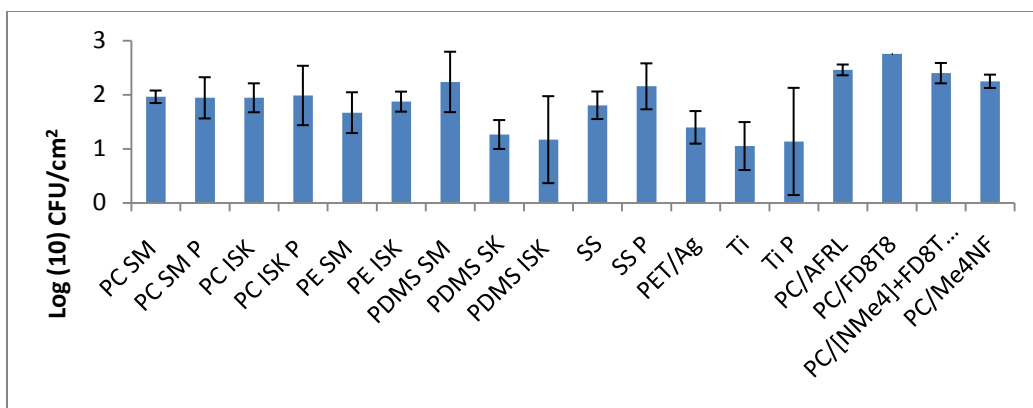


Figure 11. HPC comparison between coupons during the lunar-gravity parabolic flight (n=4).

CONCLUSION

Analysis methods indicated that the flight hardware performed nominally and that minimal variability occurred between flight and ground experiments. The short-term duration of the microgravity and lunar-gravity parabolic flights was not conducive to the advancement of biofilm formation. However, there was a slight decrease in cellular adhesion to the coupons with PDMS with both the Sharklet™ and the ISK pattern over the unpatterned surface. There was also a decrease in cells on the coupons containing an Ag coating over the control samples. Although the ATP/cell for the *P. aeruginosa* healthy terrestrial samples was similar to the anticipated benchmark for *E. coli*, exposure to short-term variable gravity caused the amount of ATP/cell to more than double—an effect that was greater in the lunar-gravity flight samples. As anticipated, the amount of ATP per cell decreased when exposed to either formalin or Ag fixation. For both flight and ground experiments, fixing with formalin had an increased negative impact on cellular metabolism over Ag fixation.

Further evaluation will be conducted on optimizing the ATP method for coupon surfaces and to confirm whether the increased ATP found in the lunar-gravity flight over the microgravity flight is specific to flight conditions or time dependent. Further experiments need to be performed at longer durations of reduced gravity to extrapolate the microgravity and 2-gravity segments of the parabolic data. New materials will be developed and tested in 1-gravity environments using ASTM methods to improve the materials' antimicrobial response.

ACKNOWLEDGEMENTS

The principal investigators would like to thank the integrated phase planning (IPP) FAST program for providing them an opportunity to perform reduced-gravity experiments aboard the Zero-G aircraft. We would also like to thank the KSC IPP office for its financial support for funding the use of shuttle flight hardware for the experiment.

This report is submitted as part of a requirement of the NASA IPP FAST Reduced Gravity Program.

The following table describes the materials in this article as well as provides the materials' source/vendor.

Materials	Description	Source/Vendor
PC SM	Polycarbonate, smooth	Sharklet Technologies, Inc.
PC SM P	PC with pilin peptide, smooth	Sharklet Technologies, Inc.
PC ISK	PC with inverse Sharklet™ pattern	Sharklet Technologies, Inc.
PC ISK P	PC with inverse Sharklet™ pattern and pilin peptide	Sharklet Technologies, Inc.
PC/AFRL	Polycarbonate (AFRL)	Air Force Research Laboratory
PC/FD ₈ T ₈	PC + [10% fluorodecyl polyhedral oligomeric silsesquioxane] (ie, polycarbonate with fPOSS)	Air Force Research Laboratory
PC/[NMe ₄] ⁺ FD ₈ T ₈	PC + [10% Me ₄ N ⁺ fPOSS(F)] (ie, polycarbonate with caged fPOSS)	Air Force Research Laboratory
PC/Me ₄ NF	PC + [0.25% Me ₄ N ⁺ F ⁻] (ie, polycarbonate with cage but no fPOSS)	Air Force Research Laboratory
PDMS SM	polydimethylsiloxane elastomer, smooth	Sharklet Technologies, Inc.
PDMS SK	PDMS with Sharklet™ pattern	Sharklet Technologies, Inc.
PDMS ISK	PDMS with inverse Sharklet™ pattern	Sharklet Technologies, Inc.
PE SM	Polyethylene, smooth	Sharklet Technologies, Inc.
PE ISK	PE with inverse Sharklet™ pattern	Sharklet Technologies, Inc.
PET/Ag	Silver-coated polyethylene terephthalate	Georgia Tech Research Institute
PET/Ag P	Silver-coated PET with pilin peptide	Georgia Tech Research Institute
SS	Stainless steel 316	BioSurface Technologies Corporation (Bozeman, Mont.)
SS P	Stainless steel 316 with pilin peptide	BioSurface Technologies Corporation
Ti	Titanium 6Al-4V	BioSurface Technologies Corporation
Ti P	Titanium 6Al-4V with pilin peptide	BioSurface Technologies Corporation

REFERENCES

- Bailey TC, Johnson SC, Resnick DJ, Sreenivasan SV, Ekerdt JG, Willson CG. Step and Flash Imprint Lithography: An Efficient Nanoscale Printing Technology. *J Photopolym Sci Technol.* 2002;15(3):481.
- Bloem J. Fluorescent staining of microbes for total direct counts. In: *Molecular Microbial Ecology Manual*. The Netherlands: Kluwer Academic Publishers; 1995;4.1.8:1-12.
- Boulos L, Prevost M, Barbeau B, Callier J, Desjardins R. LIVE/DEAD BacLight: Application of a New Rapid Staining Method for Direct Enumeration of Viable and Total Bacteria in Drinking Water. *J Microbiol Meth.* 1999;37:77-86.
- Carman ML, Estes TG, Feinberg AW, et al. Engineered Antifouling Microtopographies – Correlating Wettability with Cell Attachment. *Biofouling.* 2006; 22(1):11-21.
- Cassie ABD, Baxter S. Wettability of Porous Surfaces. *Trans Faraday Soc.* 1944;40:546-551.
- Chang JH, Cheng FS, Chao CC, Weng YC, Yang SY. Direct Imprinting Using Soft Mold and Gas Pressure for Large Area and Curved Surfaces. *J Vac Sci Technol.* 2005;A23(6):1687-1690.
- Chang JH, Yang SY. Gas Pressurized Hot Embossing for Transcription of Micro-features. *Microsystem Technologies.* 2003;10:76-80.
- Cheng FS, Yang SY, Chen CC. Novel Hydrostatic Pressuring Mechanism for Soft UV-imprinting Processes. *J Vac Sci Technol.* 2008; 26(1):132-136.
- Cheng FS, Yang SY, Nian SC, Wang LA. Soft Mold and Gasbag Pressure Mechanism for Patterning Submicron Patterns onto a Large Concave Substrate. *J Vac Sci Technol.* 2006;B24(4):1724-1727.
- Choi WM, Park OO. The Fabrication of Submicron Patterns on Curved Substrates Using a Polydimethylsiloxane Film Mould. *Nanotechnology.* 2004;15:1767-1770.

11. Chung KK, Schumacher JF, Pruitt JC, et al. Impact of Engineered Surface Microtopography on Biofilm Formation of *Staphylococcus aureus*. *Biointerphases*. 2007; 2(2):89-94.
12. Crombrugge J, Waes G. ATP method. In: Heeschen W, ed. *Methods for Assessing the Bacteriological Quality of Raw Milk from the Farm*. Brussels: International Dairy Federation: 1991;53-60.
13. del Campo A, Arzt E. Fabrication Approaches for Generating Complex Micro- and Nanopatterns on Polymeric Surfaces. *Chem Rev*. 2008;108:911-945.
14. den Braber ET, de Ruijter JE, Ginsel LA, von Recum AF, Jansen JA. Quantitative Analysis of Fibroblast Morphology on Microgrooved Surfaces with Various Groove and Ridge Dimensions. *Biomaterials*. 1996;17(21):2037-2044.
15. den Braber 1998, de Ruijter JE, Ginsel LA, von Recum AF, Jansen JA. Orientation of ECM Protein Deposition, Fibroblast Cytoskeleton, and Attachment Complex Components on Silicone Microgrooved Surfaces. *J Biomed Mater Res*. 1998;40(2):291-300.
16. Gates BD, Xu Q, Stewart M, Ryan D, Willson CG, Whitesides GM. New Approaches to Nanofabrication: Molding, Printing, and Other Techniques. *Chem Rev*. 2005;105:1171-1196.
17. Gregori G, Citterio S, Ghiani A, et al. Resolution of Viable and Membrane-compromised Bacteria in Freshwater and Marine Waters Based on Analytical Flow Cytometry and Nucleic Acid Double Staining. *Appl Environ Microbiol*. 2001;67:4662-4670.
18. Haatainen T, Majander P, Kela T, Ahopelto J, Kawaguchi Y. Imprinted 50 nm Features Fabricated by Step and Stamp UV Imprinting. *Jpn J Appl Phys*. 2008;47(6):5164-5166.
19. Hampp R, Hoffmann E, Schonherr K, Johann P, Filippis L. Fusion and Metabolism of Plant Cells as Affected by Micro gravity. *Planta*. 1997;203:S42-S53.
20. Hobbie JE, Daley RJ, Jasper S. Use of Nucleopore Filters for Counting Bacteria By Fluorescence Microscopy. *Appl Environ Microbiol*. 1977;33:1225-1228.
21. Kim S, Kang S. Replication Qualities and Optical Properties of UV-moulded Microlens Arrays. *J Phys D: Appl Phys*. 2003;36:2451-2456.
22. Kim YS, Suh KY, Leea HH. Fabrication of Three-dimensional Microstructures by Soft Molding. *App Phys Lett*. 2001;79:2285-2287.
23. Kunnavaakkam M, Houlihan FM, Schlax M, et al. Low-cost, Low-loss Microlens Arrays Fabricated by Soft-lithography Replication Process. *Appl Phys Lett*. 2003; 82(8):1152-1154.
24. Makela T, Haatainen T, Majander P, Ahopelto J, Lambertini V. Continuous Double-Sided Roll-to-Roll Imprinting of Polymer Film. *Jpn J Appl Phys*. 2008;47(6):5142-5144.
25. Paul KE, Prentiss M, Whitesides GM. Patterning Spherical Surfaces at the Two-Hundred-Nanometer Scale. *Adv Funct Mater*. 2003;15:259-263.
26. Ruchhoeft P, Colburn M, Choi B, et al. Patterning Curved Surfaces: Template Generation by Ion Beam Proximity Lithography and Relief Transfer by Step and Flash Imprint Lithography. *J Vac Sci Technol*. 1998;B17(6):2965-2969.
27. Rudschuck ST, Hirsch D, Zimmer K, et al. Replication of 3D-Micro- and Nanostructures Using Different UV-curable Polymers. *Microelectronic Engineering*. 2000;53:557-560.
28. Schmidt JA, von Recum AF. Texturing of Polymer Surfaces at the Cellular Level. *Biomaterials*. 1991;12(4):385-389.
29. Schumacher JF, Carman ML, Estes TG, et al. Engineered Antifouling Microtopographic Effect of Feature Size, Geometry, and Roughness on Settlement of Zoospores of the Green Alga *Ulva*. *Biofouling*. 2007A;23(1):55-62.

30. Schumacher JF, Aldred N, Callow ME, et al. Species-specific Engineered Antifouling Topographies – Correlations Between the Settlement of Algal Zoospores and Barnacle Cyprids. *Biofouling*. 2007B;23(5):307-317.
31. Schumacher JF, Long CJ, Callow ME, Finlay JA, Callow JA, Brennan AB. Engineered Nanoforce Gradients for Inhibition of Settlement (Attachment) of Swimming Algal Spores. *Langmuir*. 2008;4(9):4931-4937.
32. Suho A, Cha J, Myung H, et al. Continuous Ultraviolet Roll Nanoimprinting Process for Replicating Large-scale Nano- and Micropatterns. *Appl Phys Lett*. 2006;89:213101-213103.
33. Suho A, Minseok C, Hyungdae B, et al. Design and Fabrication of Micro Optical Film by Ultraviolet Roll Imprinting. *Jpn J Appl Phys*. 2007;46(8b):5478-5484.
34. Tanaka H, Matsumoto K, Shimoyama I. Fabrication of a Three-dimensional Insect-wing Model by Micromolding of Thermosetting Resin with a Thin Elastomeric Mold. *J Micromech Microeng*. 2007;17: 2485-2490.
35. van Kooten TG, Whitesides JF, von Recum AF. Influence of Silicone (PDMS) Surface Texture on Human Skin Fibroblast Proliferation as Determined by Cell Cycle Analysis. *J Biomed Mater Res*. 1998;43(1):1-14.
36. van Kooten TG, von Recum AF. Cell Adhesion to Textured Silicone Surfaces: The Influence of Time of Adhesion and Texture on Focal Contact and Fibronectin Fibril Formation. *Tissue Eng*. 1999;5:223-240.
37. Xia Y, Whitesides GM. Soft Lithography. *Annu Rev Mater Sci*. 1998;28:153-184.

PHOTOGRAPHS

None available.

VIDEO

- Zero G flight week 8/11 – 8/14, 2009 Master/TSR: 103823

Videos are available from Imagery and Publications Office (GS4), NASA JSC.

CONTACT INFORMATION

Luke Roberson, PhD
 Research Scientist
 Mail Code: NE-L6-P
 NASA Kennedy Space Center, FL 32815

TITLE

Education Outreach Program –
Space Motion Sickness and the Semicircular Canals of the Inner Ear

PRINCIPAL INVESTIGATORS

Matthew Allner
Rich Simonsen

COINVESTIGATOR

Paul Uranga, NASA Johnson Space Center, Houston, TX, Mentor

FLIGHT DATES

April 26–30, 2010



GOAL

Fluids of different viscosities flow at different rates in a 1-gravity environment. This investigation will attempt to determine whether these same fluids flow at different rates while in a simulated microgravity environment.

OBJECTIVES

This experiment was designed by students at Fox Meadow Middle School in Colorado Springs, CO. The students were learning about space adaptation syndrome (SAS)/space motion sickness (SMS) in their NASA space science class and wanted to better understand why so many astronauts experience SMS symptoms during their first few days of spaceflight. These students thought that building a model of the inner ear and the semicircular canals would allow them to better visualize what really happens with endolymph fluid movement. Students were also curious whether fluids of different viscosities would flow differently through semicircular, canal-shaped tubes when exposed to a reduced-gravity environment.

The question these students wanted answered was: *What implication does the experiment have for understanding the astronaut's inner ear?* The endolymph fluid of the semicircular canals of the inner ear moves in 1 G as the head is moved in all three axes (x, y, and z). In microgravity, this fluid moves freely due to the altered state of gravity, thus contributing to the Conflict Theory that causes SMS (Churchill, 1997; Connors, Harrison, and Akins, 2005). Our flight experiment design will allow us to collect data on how three different liquids (of differing viscosities) move in a simulated space environment. We feel that the fluid that is probably most like the endolymph fluid is vegetable oil because it tends to move more freely than the other two fluids. However, the reason for us investigating the other two fluids (dish soap and syrup) is that we are curious as to whether the endolymph fluid viscosity of astronauts, who will be living permanently in altered-gravity environments, will change to allow their bodies to adapt to the environment in which they will be living. We think this fluid could thicken in time; hence, we are also studying two other fluids that are slightly more viscous than endolymph fluid.

METHODS AND MATERIALS

We anticipate that by using clear plastic tubing that is calibrated and mounted in various positions, we will be able to measure flow rates during periods of microgravity as well as the rate of return (resettling of the liquid) during hypergravity.

The original design is a model of the three axes of rotation and the semicircular canals of the inner ear (figure 1). To generate sufficient post-flight data analysis, two more experiments were built: the primary experiment, which will be designed for the flight (figure 2), and a second experiment, which will serve as a prototype to allow us to test the fluids and collect data in the classroom (figure 3). The data collected from the in-class experiment will then be cross-analyzed with data collected during the flight in an effort to provide a post-flight analysis and lessons learned.

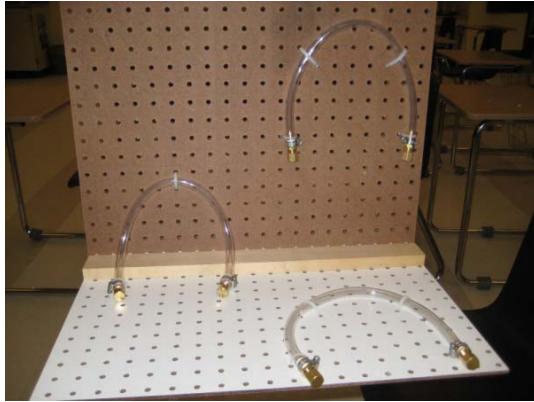


Figure 1. SMS FOX FT 2 – flight experiment.



Figure 2. SMS FOX FT 2 – in-flight experiment.

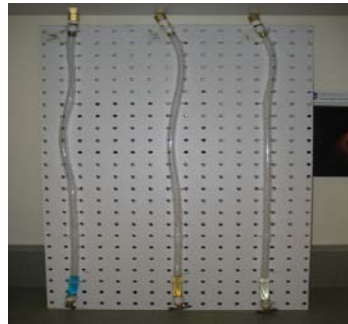


Figure 3. SMS FOX FT 1 – class experiment.

We will be measuring the distance that three different fluids (vegetable oil, dish soap, and syrup) will flow through 0.5-in. vinyl tubing. Assuming the fluids will move when in microgravity/zero gravity, the maximum length of tubing that any one fluid can move will be 28 cm. We will be calibrating the tubing to record the amount of movement of each liquid; using periods of microgravity, we will be recording the time it takes for the liquids to either flow all the way to the opposite end or the time it takes for the parabola to be completed.

We anticipate that the flow rates of the three selected liquids will vary when tested on Earth. The flow rate of each liquid will remain consistent in microgravity, but the distances the liquids may travel and their velocities in the tubing may vary. Our assumption was based on the premise that in positive gravity, downward force and the acceleration rate of an object are constant. Since a small amount of gravitational force is still present in microgravity we feel the flow rates will remain in the same order as tested on Earth, but will be slower due to the reduction of gravitational force.

Again, one side of our experiment will be for the data collection portion and the other will be a model of the semicircular canals of the inner ear, displaying three tubes with one in each of the three axes (x, y, and z). Each of these three tubes will have vegetable oil in them (simulating the endolymph fluid).

The following is a list of the equipment to be brought on board the aircraft. All equipment will be stowed in a Reduced Gravity Office (RGO) glove box for takeoff and landing. The camera pole used for mounting the video camera will be in place and bolted to the floor during takeoff and

landing; but the camera itself will be attached after takeoff. The total weight of all experiment components is approximately 13 lb, not including the RGO glove box.

Space Motion Sickness Fluid Tester (SMS-FOX-FT 2)

The following comprise the parts of the figure 1 flight experiment:

1. Experiment assembly
 - 12 hose barb adapter caps
 - 12 hose barb adapters (3/8 in. × 1/4 in.)
 - 9 vinyl plastic tubing pieces
 - 40 small plastic zip ties (10 cm)
 - 6 drain cock valves (1/4 in.)
 - 3 fluids for testing Dawn[®] dish soap (Proctor & Gamble, Cincinnati, OH), vegetable oil, syrup
 - 18 pieces of plumber's tape (each 17-cm long)
 - Peg board
 - One 4-in. metal hinge
 - 2 wing nuts
 - Wood-threaded shaft
 - Grooved piece of maple wood (for the divider)
 - Various small scraps of pine wood
 - 30 wood screws
 - Two 1/4-in. nuts and bolts with 2 washers each
 - 18 hose clamps
2. Three camera mounts, attached preflight
3. Two digital video cameras
4. One digital camera (ie, still camera)
5. RGO glove box
6. One spinning top, 1 U.S. penny, and 1 Slinky[®] (POOF-Slinky, Inc., Plymouth, MI) – Educational outreach experiment
7. Three spare batteries

All equipment was stowed in the RGO glove box for takeoff and landing. The flight team will ensure that all equipment is properly secured and stored within the crates before takeoff and landing. The glove box attachment will be inspected before takeoff and landing to ensure it is correctly fastened to the aircraft floor.

SMS FOX FT2 – In-flight (1 G)

1. During zero-g – Flier 1 will be positioned on the hinge side (ie, the bottom) of the experiment, and Flier 2 will sit to either side of the experiment. Flier 1 will watch the movement of the liquids and the distance the liquids travel. He/she will also note both the time and the distance the liquids are moving and this information will be recorded in a data table. Flier 2 will run the stop watch for the first half of the testing (seven parabolas); his/her job will be to (1) call out the test number as the test begins and (2) give Flier 1 the time at which Flier 1 sees a liquid has reached the end of the tubing. After the seventh parabola, Flier 1 and Flier 2 will switch places and will continue collecting data the same as before, but for eight more parabolas.

2. During hypergravity, the board will always be set back at 90 deg to assist with fluid re-settling. On receiving a call (announcement) that they will be coming out of hypergravity, Flier 1 and Flight 2 will then readjust the board back to the desired angle. Flier 1 will sit as still as possible but will monitor the board to see how much of the liquids resettle.
3. At least 15 parabolas will be used to collect data; we would like to set the adjustable peg board at the following three angles: 0, 45, and 90 deg. We plan on running five trials during which the board is at each angle.
4. During each test, a video camera will be set up to tape both sides of the experiment. Thus, if any data are miscalculated or unobserved, we can catch the miscalculation or unobserved occurrence on film during the post-flight review with students.

RESULTS

Classroom Data

Results from our classroom experiment prototype were first collected in the classroom; these are shown in figures 4a and 4b.

Microgravity Simulation (8-deg decline)

Blue							
Liquid	Flow Distance (cm)	Time (sec)					Avg Time
		Trial 1	Trial 2	Trial 3	Trial 4	Trial 5	
Veg. Oil	53	34.28	29.44	24.84	29.72	34	30.456
Syrup	53	190.01	300	403	271	364	305.602
Dish Soap	53	262	231	221	238	200	230.4

Red							
Liquid	Flow Distance (cm)	Time (sec)					Avg Time
		Trial 1	Trial 2	Trial 3	Trial 4	Trial 5	
Veg. Oil	54	34.6	40.61	40.61	29.37	54.81	40
Syrup	54	277.03	468.72	557.59	495.79	783.97	516.62
Dish Soap	54	428.69	263.22	243.57	206	241.03	276.502

Figure 4a. Microgravity simulation data (8-deg decline). Classroom data were collected from two separate student groups (Blue Team and Red Team),

Earth (1 G) Data Collection

Blue

Liquid	Flow Distance (cm)	Time (sec)					Avg Time
		Trial 1	Trial 2	Trial 3	Trial 4	Trial 5	
Veg. Oil	53	5	8	5.38	7.25	5.16	6.158
Syrup	53	53	38	32.5	53.85	41.63	43.796
Dish Soap	53	25	31	25	31	21.84	26.768

Red

Liquid	Flow Distance (cm)	Time (sec)					Avg Time
		Trial 1	Trial 2	Trial 3	Trial 4	Trial 5	
Veg. Oil	54	4.84	2.88	6.38	7.25	5.25	5.32
Syrup	54	62.25	88.03	64.96	87.13	60.56	72.586
Dish Soap	54	22.9	25.6	24.91	28.71	22.44	24.912

Figure 4b. 1g classroom data. Liquids movement was measured when experiment board was in a 90-deg angle, perpendicular to the ground.

In Earth-based analyses conducted on humans, bed rest studies have provided numerous useful insights into many of the physiological responses humans would have in the space environment (Connors, Harrison, and Akins, 2005). Such studies involve using human subjects and placing them in a head-down tilt position for various lengths of time while physiological processes were monitored and countermeasures were implemented in efforts to better learn how to best improve astronaut health while in the microgravity environment of space. Following this idea of a bed rest study, we hypothesized that an 8-deg downward tilt (decline) would possibly produce results that would be similar to those obtained in bed rest studies as well as in a microgravity environment.

Students recorded data from two separate experiment test boards. Five trials were completed by each student group. Figure 4a indicates movement of all three liquids, with syrup moving the slowest and vegetable oil moving the fastest after five trials. Looking at the data in figure 4b, the same pattern exists in that syrup moved the slowest and vegetable oil moved the fastest.

Flight Day 1 Data

Results from our flight experiment design were collected on two separate flights and shown in figures 5a through 5e (Flight Day 1) and figures 6a and 6b (Flight Day 2). Unfortunately, due to the lack of movement during both flights, it was difficult to collect significant data to support our hypothesis, as well as to accumulate data in which to engage in any sort of intelligent discussion and formulation of conclusions.

RGO Flight (90-deg incline)

Liquid	Parabola Tests 1, 2, and 3							
	(Microgravity)				Hypergravity			
	Distance (cm)		Time (sec)		Distance (cm)		Time (sec)	
Veg. Oil	5	5	0	15	5	5	0	15
Syrup	2	2	0	15	2	2	0	15
Dish Soap	3	3	0	15	3	3	0	15

Figure 5a. Flight Day 1 – Parabola Test 1, 2, and 3 (90-deg incline).

RGO Flight (45-deg incline)

Liquid	Parabola Tests 1, 2, and 3							
	(Microgravity)				Hypergravity			
	Distance (cm)			Time (sec)	Distance (cm)			Time (sec)
Veg. Oil	5	5	0	15	5	5	0	15
Syrup	2	2	0	15	2	2	0	15
Dish Soap	3	3	0	15	3	3	0	15

Figure 5b. Flight Day 1 – Parabola Test 1, 2, and 3 (45-deg incline).

RGO Flight (0-deg incline)

Liquid	Parabola Test 1							
	(Microgravity)				Hypergravity			
	Distance (cm)			Time (sec)	Distance (cm)			Time (sec)
Veg. Oil	8	10	2	15	8	12	4	15
Syrup	10	11	1	15	11	12	1	15
Dish Soap	9	11	2	15	9	12	3	15

Figure 5c. Flight Day 1 – Parabola Test 1 (0-deg incline).

Liquid	Parabola Test 2							
	(Microgravity)				Hypergravity			
	Distance (cm)			Time (sec)	Distance (cm)			Time (sec)
Veg. Oil	9	12	3	15	8	11	3	15
Syrup	11	12	1	15	11	13	2	15
Dish Soap	10	14	4	15	11	14	3	15

Figure 5d. Flight Day 1 – Parabola Test 2 (0-deg incline).

Liquid	Parabola Test 3							
	(Microgravity)				Hypergravity			
	Distance (cm)			Time (sec)	Distance (cm)			Time (sec)
Veg. Oil	11	16	5	15				15
Syrup	6	9	3	15				15
Dish Soap	6	17	9	15				15

Figure 5e. Flight Day 1 – Parabola Test 3 (0-deg incline).

Flight Day 2 Data

Results from Flight 2 tests produced the results shown in figures 6a and 6b.

RGO Flight (90-deg incline)

Liquid	Parabola Tests 1 and 2							
	(Microgravity)				Hypergravity			
	Distance (cm)			Time (sec)	Distance (cm)			Time (sec)
Veg. Oil	5	5	0	15	5	5	0	15
Syrup	2	2	0	15	2	2	0	15
Dish Soap	3	3	0	15	3	3	0	15

Figure 6a. Flight Day 2 – Parabola Tests 1 and 2 (90-deg incline).

Liquid	Parabola Test 3							
	(Microgravity)				Hypergravity			
	Distance (cm)			Time (sec)	Distance (cm)			Time (sec)
Veg. Oil	5	2	0	15	5	5	0	15
Syrup	2	2	0	15	2	6	4	15
Dish Soap	3	3	0	15	3	3	0	15

Figure 6b. Flight Day 2 – Parabola Test 3 (90-deg incline).

The comparison of data from figures 4a and 4b to those of figures 5a through 5e and 6a and 6b indicates differentiation in fluid movement. Figures 5a through 5e indicate that the only movement in any liquid occurred when the board was set in the 0-deg setting (figures 5c, 5d, and 5e). How much of this movement was due to simple displacement as opposed to any change in gravity is questionable, however. Further analysis of why no movement took place during the 45- and 90-deg settings was hypothesized as being due to the fact that the tube pressure was not vented on reaching the flight experiment cruising altitude. Following Flight Day 1, the fliers discussed this possibility and decided on Flight Day 2 to vent all six tubes on the hinge side of the pegboard. Results of the venting (figures 6a and 6b) led to more fluid movement, but the movement was not continuous and consistent as anticipated and as observed during the classroom tests, especially with the dish soap. During the 90-deg setting, while fluid movement was seen in the soap, what was visible in the tube was separated by pockets of air, which made it difficult to accurately measure displacement. Interestingly, during hypergravity any movement of the soap that did occur resulted in a lack of complete resettling back to the starting point of the liquid. It was difficult to say, from the data we were able to collect, that one liquid tended to move farther than another liquids. Data results were very inconsistent.

DISCUSSION

Analysis of our data showed that while we were able to collect some relevant data after modifications following Flight Day 1, the data results were not similar to those we collected in the classroom. Although our experiment did work after venting the tubes, the movement of liquid was still much less in microgravity than in the simulated microgravity setting (ie, the 8-deg downward tilt) we created in the classroom.

CONCLUSION

From our hypothesis and efforts in this investigation, we conclude that our experiment was a success. Although it did not work the way we had predicted, we considered the experiment a success because of the results we were able to collect. Although inconsistent, the data collected in flight showed us how unpredictable fluid movement can be in a microgravity (or simulated microgravity) environment. It is also possible that the lack of fluid movement in the experiment during both days of flight might have provided some evidence of the conflict theory. By this we mean that our test subject reported that during flight his body consistently would sense the simulated microgravity environment each time a parabola was flown, while sensing the hypergravity environment as well. However, the test subject did not recall anything out of the ordinary with regards to visual changes or disturbances providing any input out of the ordinary. Assuming that the fluid in the inner ear either moves or does not move much (as in our experiment), a conflict of information could have been taking place during simulated microgravity flights such as RGO; this may have resulted in differences in information being sent to the brain, as opposed to what it

is accustomed to receiving for input in a 1-gravity environment. This would most likely explain why a conflict takes place between the inner ear and the brain during spaceflight, leading to the development of SMS (Churchill, 1997).

BIBLIOGRAPHY

1. Churchill SE. *Fundamentals of Space Life Sciences*. Malabara, FL: Krieger Publishing Company, Inc., 1997;pp. 167-168.
2. Connors MM, Harrison AA, Akins FR. *Living Aloft*. Honolulu, HA: University Press of the Pacific, 2005;36:21-25.

PHOTOGRAPHS

J SC2010E060420 to JSC2010E060423
J SC2010E060436 to JSC2010E060438
JSC2010E060847 to JSC2010E060853
JSC2010E060856 to JSC2010E060857
JSC2010E060873
JSC2010E060883 to JSC2010E060885
JSC2010E060893 to JSC2010E060895
J SC2010E060897

VIDEO

- Zero G flight week 23 – 30 April, 2010 Master: 882773, 882774, 882775

Videos are available from Imagery and Publications Office (GS4), NASA JSC.

ACKNOWLEDGEMENTS

We would like to thank the following individuals and organizations for their support with the development and flight of our project: The mathematics, engineering, science, and achievement (MESA) program at Harrison School District; all MESA participants (David Davidson, Darius Casaus, Steven Varney, Selena Quintanilla, Rebecca Cos, Melissa Arnold, Natalie and Marselino Padilla, Amy Shrieves, Brandee Lantz, James Hoovestol, and Preston Bolyard); Fox Meadow Middle School; The Home Depot, Inc. (Atlanta, GA); the NASA Explorer School Program; the National Science Teachers Association (NSTA); our NASA Mentor Mr. Paul Uranga; and our MESA coordinators Mr. Allner and Mr. Simonsen.

CONTACT INFORMATION

Paul Uranga
Paul.uranga1@nasa.gov

Appendix

Background Information about the C-9 and the Reduced Gravity Program

The Reduced Gravity Program, operated by NASA JSC, provides engineers, scientists, and astronauts alike a unique opportunity to perform testing and training in a weightless environment but without having to leave the confines of the Earth's orbit. Given the frequency of space shuttle missions and the construction and habitation of the ISS, the Reduced Gravity Program provides an ideal environment in which to test and evaluate space hardware and experimental procedures prior to launch.

The Reduced Gravity Program was established in 1959 to investigate the reactions of humans and hardware during operations in a weightless environment. A specially modified turbojet that flies parabolic arcs produces periodic episodes of weightlessness lasting 20 to 25 s. The aircraft is sometimes also flown to provide short periods of lunar (1/6) and Martian (1/3) gravity. Over the last 50 years, in excess of 100,000 parabolas have been flown in support of the Mercury, Gemini, Apollo, Skylab, Space Shuttle, and ISS Programs.

Excluding the C-9 Flight Crew and the Reduced Gravity Program Test Directors, NASA's C-9 aircraft accommodates seating for a maximum of 20 other passengers. The C-9's cargo bay provides a test area that is approximately 45 ft long, 104 in. wide, and 80 in. high.

NASA has also transitioned to using Zero G Corporation's (Vienna, VA) 727 aircraft, which will hold up to 30 investigators. Zero G Corporation's 727 is nearly identical in size and volume to the KC-135 aircraft previously used by NASA to support the Reduced Gravity Program. The Zero G Corporation's Boeing 727 has a larger cargo door than the KC-135 that accommodates large payloads and provides a test areas that is approximately 70 ft long, 140 in. wide, and 86 in. high.

Both aircraft are equipped with electrical power for test equipment and photographic lights. When requested, professional photography and video support can be scheduled to document activities in flight.

A typical flight lasts 2 to 3 h and consists of 30 to 40 parabolas. The parabolas are flown in succession or with short breaks between maneuvers to allow time for reconfiguration of test equipment.

For additional information concerning flight weeks sponsored by JSC's Human Adaptation Countermeasures Division or other Reduced Gravity Program opportunities, please contact:

Todd Schlegel, MD
Technical Monitor, Human Adaptation
and Countermeasures Division
NASA Lyndon B. Johnson Space Center
Mail Code: SK
Houston, TX 77058
Telephone: (281) 483-9643

Dominic Del Rosso
Test Director
NASA Lyndon B. Johnson Space Center
Reduced-Gravity Office, Ellington Field
Mail Code: CC43
Houston, TX 77034
Telephone: (281) 244-9113

Explore the Zero Gravity Experiments and Aircraft Operations Web pages at:

<http://zerog.jsc.nasa.gov/>

<http://jsc-aircraft-ops.jsc.nasa.gov>

REPORT DOCUMENTATION PAGE			Form Approved OMB No. 0704-0188	
Public reporting burden for this collection of information is estimated to average 1 hour per response, including the time for reviewing instructions, searching existing data sources, gathering and maintaining the data needed, and completing and reviewing the collection of information. Send comments regarding this burden estimate or any other aspect of this collection of information, including suggestions for reducing this burden, to Washington Headquarters Services, Directorate for Information Operations and Reports, 1215 Jefferson Davis Highway, Suite 1204, Arlington, VA 22202-4302, and to the Office of Management and Budget, Paperwork Reduction Project (0704-0188), Washington, DC 20503.				
1. AGENCY USE ONLY (Leave Blank)	2. REPORT DATE September 2010	3. REPORT TYPE AND DATES COVERED Technical Memorandum		
4. TITLE AND SUBTITLE C-9 and Other Microgravity Simulations – Summary Report			5. FUNDING NUMBERS	
6. AUTHOR(S) Space Life Sciences Directorate, Human Adaptation and Countermeasures Division, NASA Johnson Space Center				
7. PERFORMING ORGANIZATION NAME(S) AND ADDRESS(ES) Lyndon B. Johnson Space Center Houston, Texas 77058			8. PERFORMING ORGANIZATION REPORT NUMBERS S-1078	
9. SPONSORING/MONITORING AGENCY NAME(S) AND ADDRESS(ES) National Aeronautics and Space Administration Washington, DC 20546-0001			10. SPONSORING/MONITORING AGENCY REPORT NUMBER TM-2010-216132	
11. SUPPLEMENTARY NOTES *NASA Johnson Space Center				
12a. DISTRIBUTION/AVAILABILITY STATEMENT Unclassified/Unlimited Available from the NASA Center for AeroSpace Information (CASI) 7115 Standard Drive Hanover, MD 21076-1320 Category: 52			12b. DISTRIBUTION CODE	
13. ABSTRACT (Maximum 200 words) This document represents a summary of medical and scientific evaluations conducted aboard the C-9 and other NASA-sponsored aircraft from June 2009 to June 2010. Included is a general overview of investigations manifested and coordinated by the Human Adaptation and Counter-measures Division. A collection of brief reports that describe tests conducted aboard the NASA-sponsored aircraft follows the overview. Principal investigators and test engineers contributed significantly to the content of the report, describing their particular experiment or hardware evaluation. Although this document follows general guidelines, each report format may vary to accommodate differences in experiment design and procedures. This document concludes with an appendix that provides background information concerning the Reduced Gravity Program.				
14. SUBJECT TERMS weightlessness; weightlessness simulation; parabolic flight; zero gravity; aerospace medicine; astronaut performance; bioprocessing; space manufacturing			15. NUMBER OF PAGES 56	16. PRICE CODE
17. SECURITY CLASSIFICATION OF REPORT Unclassified	18. SECURITY CLASSIFICATION OF THIS PAGE Unclassified	19. SECURITY CLASSIFICATION OF ABSTRACT Unclassified	20. LIMITATION OF ABSTRACT Unlimited	
